

Table of Contents

2014 International Conference on Enzyme (ICE 2014).....	2
2014 International Conference on Catalysis (ICC 2014).....	6
The 3 rd Int'l Conf. on Geology and Geophysics (ICGG 2014) & The 2 nd Hydrology, Ocean and Atmosphere Conference (HOAC 2014) & The 3 rd International Conference on New Energy and Sustainable Development (NESD 2014).....	10
The 2nd Genetics and Genomics Conference (GC 2014) & the 2 nd Int'l Conf. on Biomedical Engineering (ICBE 2014)	20
Appendix	23
ICE 2014	23
Oral Session	233
ICC 2014	31
Oral Session I.....	31
Oral Session II.....	36
ICGG 2014 & HOAC 2014 & NESD 2014.....	42
Oral Session I.....	42
Oral Session II.....	52
GC 2014 & ICBE 2014.....	64
Oral Session	64
Instructions for Presentations.....	72
Hotel Information.....	73
Contact Us.....	74

2014 International Conference on Enzyme (ICE 2014)

Schedule

Registration (June 13-15, 2014)

Location: Lobby, Beijing Yanshan Hotel

Time: June 13, 14:00 - 17:00

Location: 2nd floor, Beijing Yanshan Hotel

Time: June 14, 08:30 - 12:00

Oral Session I (June 14, 2014)

Location: Function Room (晴雪厅), 2nd floor, Beijing Yanshan Hotel

Time: 08:30-12:00 (Coffee Break 10:30-10:45)

➤ **Invited Speech:** Mechanistic Insights into Collagen Degradation by Collagenolytic Serine Protease in the Subtilisin Family

Speaker: Prof. Xiu-Lan Chen, Shandong University, China

Time: 08:30-09:00

Lunch

Location: VISTA CAFÉ (雅景咖啡厅), 1st Floor, Beijing Yanshan Hotel

Time: June 14, 12:00-13:30

Dinner

Location: VISTA CAFÉ (雅景咖啡厅), 1st Floor, Beijing Yanshan Hotel

Time: June 14, 18:30-19:30

One-day Tour (at own expense)

Location: The Great Wall and Ming Tombs (Thirteen Tombs of Ming Dynasty)

Time: June 15, 2014

Invited Speeches

Invited Speech: Numerical Dissipation and Wrong Propagation Speed of Discontinuities for Stiff Reactive Flows

Speaker: Prof. Xiu-Lan Chen, Shandong University, China

Time: 08:30-09:00, Saturday Morning, June 14, 2014

Location: Function Room (晴雪厅), 2nd floor, Beijing Yanshan Hotel



Abstract

The S8 family, also known as the subtilisin family, is the second largest family of serine proteases. Most S8 proteases are secreted endopeptidases from bacteria. While a majority of S8 proteases cannot degrade collagen, in recent decades, a number of S8 proteases from both environmental and pathogenic microorganisms have been reported to be collagenolytic proteases. By far, the collagenolytic mechanism of these S8 proteases is still unclear. Collagen is enriched in marine animals. Because collagen is water insoluble, it should be an important component of organic nitrogen in marine sediments. Therefore, collagen degradation is an important part of nitrogen recycling in marine sediments. In recent years, we purified and characterized several S8 collagenolytic proteases from the bacteria isolated from deep-sea sediments, such as deseasin MCP-01 from *Pseudoalteromonas* sp. SM9913 and myroiclsin from *Myroides profundus* D25. These S8 collagenolytic proteases are novel multidomain proteases with domain structures different from other S8 proteases. By using SEM and AFM observation, as well as structural, biochemical and mutational analyses, the collagen degradation mechanism of these S8 collagenolytic proteases was studied in detail. Our result indicated that an enlarged substrate-binding pocket is necessary for collagen recognition and that the acidic and aromatic residues on these loops form a negatively charged, hydrophobic environment for collagen binding in these proteases. These proteases have various but specific cleavage sites triple-helical collagen molecules. Our study gives structural and mechanistic insights into collagen degradation of the S8 collagenolytic proteases, which is helpful in developing therapeutics for diseases with S8 collagenolytic proteases as pathogenic factors and in studying marine organic nitrogen degradation mechanisms.

Oral Sessions

Oral Session I

Session Chair: Prof. Suresh P.K. VIT UNIVERSITY

Invited Speaker: Prof. Xiu-Lan Chen, Shandong University, China

Function Room (晴雪厅), 2nd floor

Saturday, June 14

ID	Paper Title	Speaker	Affiliation	Time
40372	Decolorization and Preliminary analyte profiling of synthetic, organic, model, textile dyes using crude fungal laccase from <i>Rigidoporus</i> sp. cultivated with wheat bran as solid agro support medium.	Suresh P.K.	VIT UNIVERSITY	08:30-12:00
40314	Oral Submucous Fibrosis - Genetic Aspects of the Mechanistically-linked Enzymes and those associated with pathogenesis of this pre-malignant, fibrotic condition of the Oral Cavity	Suresh P.K.	VIT UNIVERSITY	08:30-12:00
40282	Studies on xyloglucanase during the germination of seeds of <i>Tamarindus indica</i>	SiddalingaMurt hy Kora Rudraiah	BANGALORE UNIVERSITY	08:30-12:00
40363	Characterization of esterases of <i>Tamarindus indica</i> seeds	KANTHARAJ U S	BANGALORE UNIVERSITY	08:30-12:00
40284	Enzyme kinetic equations of irreversible and reversible reactions in metabolism	Josep J. Centelles	Universitat Barcelona	de 08:30-12:00
40295	Catalytically important residues in <i>E. coli</i> 1-deoxy-D-xylulose 5-phosphate synthase	Santiago Imperial	Universitat Barcelona	de 08:30-12:00
40151	Non-classical cytochromes P450 of the CYP74 family	Svetlana Gorina	Kazan Institute of Biochemistry and Biophysics	08:30-12:00
40154	Unusual cytochrome P450 of brown alga <i>Ectocarpus siliculosus</i>	Valeriia Ermilova	Kazan Institute of Biochemistry and Biophysics	08:30-12:00
40155	Alterations of the catalytic mechanisms of unusual cytochromes P450 as a result of site-directed mutagenesis	Yana Toporkova	Kazan Institute of Biochemistry and Biophysics	08:30-12:00
40381	New enzymatic reaction for the synthesis of a carbon-nitrogen bond	Michihiko Kobayashi	University of Tsukuba	08:30-12:00

40331	Thermostable S-adenosylhomocysteine hydrolase from <i>Thermotoga maritima</i> : Properties and its application on S-adenosylhomocysteine production with a cofactor regeneration system	Guojun Qian	Nanjing Normal University	08:30-12:00
40358	A Feasibility Study on Production and Application of Thermostable Laccase and Xylanase in Pulp Biobleaching	Hongcheng Wang	Biofuels Institute, Jiangsu University	08:30-12:00
40355	Prospective clinical application of thioredoxin reductase as a novel diagnostic tumor marker	Aaron Yep	Health Science Center, Peking University	08:30-12:00
40342	Methodological studies on the detection of thioredoxin reductase activities in laboratory research and clinical trials	Weiwei Ma	Health Science Center, Peking University	08:30-12:00

2014 International Conference on Catalysis (ICC 2014)

Schedule

Registration (June 13-15, 2014)

Location: Lobby, Beijing Yanshan Hotel

Time: June 13, 14:00 - 17:00

Location: 2nd floor, Beijing Yanshan Hotel

Time: June 14, 08:30 - 12:00

Oral Session I (June 14, 2014)

Location: Orchid Room (雅兰厅), 2nd floor, Beijing Yanshan Hotel

Time: 08:30-12:00 (Coffee Break 10:30-10:45)

Lunch

Location: VISTA CAFÉ (雅景咖啡厅), 1st Floor, Beijing Yanshan Hotel

Time: June 14, 12:00-13:30

Oral Session II (June 14, 2014)

Location: Orchid Room (雅兰厅), 2nd floor, Beijing Yanshan Hotel

Time: 14:00-18:00 (Coffee Break 16:00-16:15)

Dinner

Location: VISTA CAFÉ (雅景咖啡厅), 1st Floor, Beijing Yanshan Hotel

Time: June 14, 18:30-19:30

One-day Tour (at own expense)

Location: The Great Wall and Ming Tombs (Thirteen Tombs of Ming Dynasty)

Time: June 15, 2014

Oral Sessions

Oral Session I

Session Chair: Prof. Shuang-Feng Yin, Hunan University

Orchid Room (雅兰厅), 2nd floor

Saturday, June 14

ID	Paper Title	Speaker	Affiliation	Time
40086	Highly dispersed Cu-base catalyst derived from layered double hydroxides for CO Hydrogenation	Xinyou Han	Institute of Coal Chemistry, CAS	08:30-12:00
40115	A Functional Hmd Analogue That Catalyzes Heterolytic Dihydrogen Cleavage and Hydrogenation of Quinone under Mild Condition	Shuang Jiang	Collaborative Innovation Center of Chemical Scienc	08:30-12:00
40120	Enhanced Photocatalytic Hydrogen Production Rate via Controlling Surface Transition State Geometry on Selectively Exposed Pt Facet on Pt/TiO ₂	Gongxuan Lu	lanzhou Institute of Chemical Physics	08:30-12:00
40136	Preparation of a Carbon-Based Solid Acid with High Acid Density via a noval method	SiYu OuYang	Hunan Normal University	08:30-12:00
40190	Template-free synthesis of Bi ₂ O ₃ -Bi ₂ S ₃ composites of novel morphologies and their enhanced photocatalytic properties	Shuang-Feng Yin	Hunan University	08:30-12:00
40199	Air-stable organoantimony complexes: Synthesis, characterization and catalysis	Renhua Qiu	Hunan University	08:30-12:00
40268	Hierarchically structured NiO/CeO ₂ nanocatalysts templated by eggshell membranes for methane steam reforming	zhitao wang	Curtin University	08:30-12:00
40020	Catalytic combustion of acrylonitrile over 3d-transition metals (Cu, Co, Fe) or Pt/SBA-15, Cu/SBA-16 and Cu/KIT-6 mesoporous catalysts	Dongjun Shi	Beijing University of Chemical Technology	08:30-12:00
40021	An Economical Way to Synthesize SSZ-13 for an Extraordinary Performance in Selectively Catalytic Reduction (SCR) of NO _x by ammonia	Ruinian Xu	Beijing University of Chemcial Technology	08:30-12:00
40022	Selective catalytic oxidation (SCO) of ammonia to nitrogen over mesoporous zeolite	Runduo Zhang	Beijing Unversity of Chemcial Technology	08:30-12:00

40023	Co ₃ O ₄ with different morphologies for catalytic combustion of CO and CH ₄ and investigation the role of their diverse oxygen species with oxygen isotopic exchange reaction	Ning Liu	Beijing University of Chemical Technology	08:30-12:00
40039	Effect of hard template's residues of the nanocasted mesoporous LaFeO ₃ perovskite with high surface area on methyl chloride oxidation	Peixin Li	Beijing University of Chemical Technology	08:30-12:00
40208	CO ₂ -based polyols for sustainable polyurethane foams	Thomas Müller	RWTH Aachen University	08:30-12:00
40375	Introduction 1,1'-butylenebis (3-methyl-3H-imidazol-1-ium) dihydrogen sulfate as an efficient Brønsted ionic liquid for the synthesis of tacrine analogues	Nader Ghaffari Khaligh	Research House of Professor Reza. Education Guilan	08:30-12:00

Oral Session II

Session Chair: Dr. Emrah Ozensoy

Bilkent University

Orchid Room (雅兰厅), 2nd floor

Saturday, June 14

ID	Paper Title	Speaker	Affiliation	Time
40064	CaIn ₂ O ₄ /Fe-TiO ₂ Composite Photocatalysts with Enhanced Visible Light Performance for Hydrogen Production	Jianjun Ding	University of Science and Technology of China	14:00-18:00
40074	COMPUTATIONAL HINTS IN OLEFIN METATHESIS	Albert Poater	Institut de Química Computacional i Catàlisi and D	14:00-18:00
40075	Ordered mesoporous carbon-titania composites as sonocatalysts: effects of frequency, power density, pH and catalyst loading dose	Pengpeng Qiu	Korea University	14:00-18:00
40098	Mechanism of Photocatalytic Degradation of Volatile Organic Compounds on TiO ₂ : An In-situ DRIFTS Study	Fan Zhang	University of Science and Technology of China	14:00-18:00
40177	Oxidation of Ibuprofen in sonocatalytic process by using magnetically separable TiO ₂	Kyounglim Kang	Korea Univesity	14:00-18:00
40182	Decolorization of Reactive Black 5 by Sonocatalytic Process with TiO ₂ /SWCNT Composite	Jongbok Choi	Korea Univesity	14:00-18:00

40194	Analysis of geometric condition for hydroxyl radical production by using stainless steel wire mesh as sonocatalyst in aqueous solution	Yonghyeon Lee	Korea University	14:00-18:00
40228	Preparation of nano-CoOx-C supported on silican spheres with high catalytic performance for ethylbenzene oxidation	zhigang liu	Hunan University	14:00-18:00
40251	SiC Nanomaterials: Application to Photoelectrochemical Water Splitting	Jianjun Chen	Zhejiang Sci-Tech University	14:00-18:00
40293	Enhanced Hydrogen Production by Ca-rich Bed-Material Coating on Olivine during Indirect Biomass Gasification	Remco Lancee	Eindhoven University of Technology	14:00-18:00
40116	Study on the Basic Centers and Active Oxygen Species of Solid-base Catalysts for Oxidation of iso-Mercaptans	Yufen Zhang	Beijing Environmental Protection and New Material Co. Ltd	SJ 14:00-18:00
40081	Mixed Oxides of Calcium and Zinc as Heterogeneous Catalyst in Biodiesel Production from Refined Palm Oil	Carlos Alberto Guerrero Fajardo	National University of colombia	14:00-18:00
40171	Palladium doped Perovskite-Based NO Oxidation Catalysts: The Role of Pd and B-sites for NOx Adsorption Behavior	Emrah Ozensoy	Bilkent University	14:00-18:00
40343	Niobium and Platinum-Wolframium catalysts in the conversion of furfuryl alcohol to cyclopentanone. Reaction in two steps.	Ilian Guzman Velez	University of Basque Country	14:00-18:00

**The 3rd Int'l Conf. on Geology and Geophysics (ICGG 2014) & The
2nd Hydrology, Ocean and Atmosphere Conference (HOAC 2014) &
The 3rd International Conference on New Energy and Sustainable
Development (NESD 2014)**

Schedule

Registration (June 13-15, 2014)

Location: Lobby, Beijing Yanshan Hotel

Time: June 13, 14:00 – 17:00

Location: 2nd floor, Beijing Yanshan Hotel

Time: June 14, 08:30 – 12:00

Invited Speech (June 14, 2014)

Location: Plum Blossom Room (沁梅厅), 2nd floor, Beijing Yanshan Hotel

Time: 08:30-12:00 (Coffee Break 10:30-10:45)

Session Chair: Prof. Heping Sun, Chinese Academy of Science, China

- **Invited Speech:** Recent Developments on Rock Mass Strength, Deformability and Rock Slope Stability through Case Studies drawn from Underground and Surface Excavations

Speaker: Prof. Pinnaduwa Kulatilake, University of Arizona, USA

Time: 08:30-09:00

- **Invited Speech:** Geodynamic and Structure of the Earth's Interior by Using Tidal Gravity Observations

Speaker: Prof. Heping Sun, Chinese Academy of Science, China

Time: 09:00-09:30

- **Invited Speech:** Carbon Nanotubes for Energy Storage

Speaker: Prof. Bingqing (B.Q.) Wei, University of Delaware, USA

Time: 09:30-10:00

- **Invited Speech:** Flow field designs of fuel cells: theory and applications

Speaker: Prof. Junye Wang, Athabasca University, Canada

Time: 10:00-10:30

- **Invited Speech:** Self-Organized Liquid Crystalline Nanostructures: From Energy-Saving Devices to Organic Photovoltaics
Speaker: Prof. Quan Li, Kent State University, USA
Time: 10:45-11:15

Lunch

Location: VISTA CAFÉ (雅景咖啡厅), 1st Floor, Beijing Yanshan Hotel
Time: June 14, 12:00-13:30

Oral Session I (June 14, 2014)

Location: Peony Room (牡丹厅), 2nd floor, Beijing Yanshan Hotel
Time: 13:30-18:30 (Coffee Break 16:00-16:15)

Oral Session II (June 14, 2014)

Location: Plum Blossom Room (沁梅厅), 2nd floor, Beijing Yanshan Hotel
Time: 13:30-18:30 (Coffee Break 16:00-16:15)

Dinner

Location: VISTA CAFÉ (雅景咖啡厅), 1st Floor, Beijing Yanshan Hotel
Time: June 14, 18:30-19:30

One-day Tour (at own expense)

Location: The Great Wall and Ming Tombs (Thirteen Tombs of Ming Dynasty)
Time: June 15, 2014

Invited Speeches

Invited Speech: Recent Developments on Rock Mass Strength, Deformability and Rock Slope Stability through Case Studies drawn from Underground and Surface Excavations

Speaker: Prof. Pinnaduwa Kulatilake, University of Arizona, USA

Time: 08:30-09:00, Saturday Morning, June 14, 2014

Location: Plum Blossom Room (沁梅厅), 2nd floor, Beijing Yanshan Hotel



Abstract

Most naturally occurring discontinuous rock masses comprise of intact rock interspaced with different types of discontinuities. In civil and mining engineering, the engineers face design and construction tasks associated with geotechnical systems that are in or on discontinuous rock masses. Some examples for such geotechnical systems are tunnels for hydropower and transport, dams, foundations, natural and man-made slopes, surface and underground excavations made for mineral extraction, underground caverns for oil and gas storage and hazardous waste isolation caverns. In these rock engineering systems, one comes across stability concerns of the rock structures. Rock mass strength and deformability play vital roles on stability of these structures. Rock mass strength and deformability depend on the (a) lithology, (b) discontinuity network, (c) geo-mechanical properties of the discontinuities, (d) geo-mechanical properties of the intact rock, (e) in situ stress system and (f) loading/unloading stress paths. A good understanding of rock mass strength and deformability is vital to arrive at safe and economical designs for structures built in and on rock masses. The presence of complicated discontinuity patterns, the inherent statistical nature of their geometrical parameters, and the uncertainties involved in the estimation of their geo-mechanical and geometrical properties and in-situ stress make accurate prediction of rock mass strength and deformability difficult. In discontinuous hard rock masses, rock slope stability is mainly governed by the discontinuity geometry and discontinuity strength. The most recent developments on rock mass strength, deformability and rock slope stability will be covered in this keynote presentation using some case histories drawn from underground and surface excavations in China and USA.

Invited Speech: Geodynamic and Structure of the Earth's Interior by Using Tidal Gravity Observations

Speaker: Prof. Heping Sun, Chinese Academy of Science, China

Time: 09:00-09:30, Saturday Morning, June 14, 2014

Location: Plum Blossom Room (沁梅厅), 2nd floor, Beijing Yanshan Hotel



Abstract

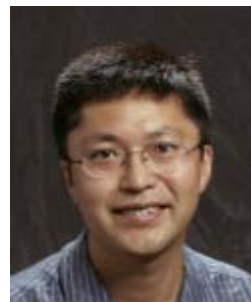
By stacking a series of high-sampling and high-precision tidal gravity observations at 25 stations in the Global Geodynamics Project (GGP) network along the world, we investigate some geodynamical problems in the Earth's Interior, including the Earth's free core nutation (FCN), Earth's free oscillation and the translational oscillation of the solid inner core. We determined important parameters including the eigen-period, quality factor (Q value) and resonance strength and so on, the environmental influence of the atmospheric pressure and oceanic loading are taken into account in data processing. The high precision tidal gravity amplitude factors are determined, the dynamic viscosity at the core-mantle boundary (CMB) is obtained for the first time based on the FCN quality factor Q values which reaches up to the order of 10^3 Pa·s, it is in good agreement with the nearest result obtained using the VLBI observations. Our results indicate that the tidal gravity is one of effective techniques for investigating the deep interior structure of the Earth.

Invited Speech: Carbon Nanotubes for Energy Storage

Speaker: Prof. Bingqing (B.Q.) Wei, University of Delaware, USA

Time: 09:30-10:00, Saturday Morning, June 14, 2014

Location: Plum Blossom Room (沁梅厅), 2nd floor, Beijing Yanshan Hotel



Abstract

Electricity storage is a growing challenge among a broad range of renewable energy sources. The development of high-energy storage devices has been one of the research areas of top most importance in recent years and rechargeable batteries and/or electrochemical capacitors (supercapacitors) are anticipated to be the primary sources of power for modern-day requirements in portable electronic devices, satellites, and electric vehicles. In the meantime, flexible/stretchable electronics have attracted considerable attention very recent years and have opened the door to many important applications that current, rigid electronics cannot achieve. In order to accommodate these needs, power source devices must be flexible and stretchable in addition to their high energy and power density, light weight, miniaturization in size, and safety requirements. Utilizing nanomaterials and nanostructures such as carbon nanotubes (CNTs) for various energy storage applications such as electrodes in lithium ion batteries and supercapacitors are under close

scrutiny because of the promising electrochemical performance of such nanomaterials. In this presentation, research efforts in assembling 2-D CNT macro-films using a chemical vapor deposition method and their applications for different energy storage devices including stretchable supercapacitors, supercapacitors working under extreme conditions such as high temperature and high pressure, and lithium-ion batteries will be discussed.

Invited Speech: Flow field designs of fuel cells: theory and applications

Speaker: Prof. Junye Wang, Athabasca University, Canada

Time: 10:00-10:30, Saturday Morning, June 14, 2014

Location: Plum Blossom Room (沁梅厅), 2nd floor, Beijing Yanshan Hotel



Abstract

Despite huge investment and efforts in the last three decades, fuel cells are still known as a fledgling industry after 170 years of the first fuel cell by Grove. There were unrealistic promises that the goals of commercialization of fuel cells were attainable and created false expectations in the public community and investors who, once again, would see a deadline come and go without the huge victory promised. Unless one really understands those challenges in commercialization there is little chance of solving them. In fact, we have no any clear idea of both theoretical solution and technical measures how to solve durability, reliability and robustness so far. There is the major challenge to transform a laboratory scale production of fuel cells to an industrial scale one and to meet the requirements of throughput, operating life, low cost, reliability and high efficiency in R&D of fuel cells. Why the simpler structure fuel cells still lag far from the steam and IC engines after massive investment in the past years? Why upscaling of fuel cells failed often when many researchers stated their successes in small scale? Surprisingly, these facts and figures are neither questioned nor discussed by expert groups and annual merit reviews. Therefore, the real cause of upscaling failures has not been realized well yet in R & D of fuel cells. Fuel cell industry faces a precipice in spite of many claimed successes. As Dr Adamson said, 'It really is do or die time in the industry. It is up to the industry itself to decide which scenario becomes reality.' Fuel cells need not tactical fixes using nano-materials or catalyst but strategic solutions. Science and technology are not for eye-catch but for practical solutions of real problems. Designs of uniform flow distribution are central to upscale fuel cells as well as to tackle critical issues of durability, robustness and reliability. Despite our growing appreciation of the uniform flow distribution in the flow field designs, a critical fact is that the designs of the uniform flow distributions are still based on empirical and qualitative approaches. In this talk, we introduce history of fuel cell development and concepts and criteria of flow field designs. Then, we present main issues and challenges to address and development of theoretical models. Finally, we discuss basic design procedure and applications.

Invited Speech: Self-Organized Liquid Crystalline Nanostructures: From Energy-Saving Devices to Organic Photovoltaics

Speaker: Prof. Quan Li, Kent State University, USA

Time: 10:45-11:15, Saturday Morning, June 14, 2014

Location: Plum Blossom Room (沁梅厅), 2nd floor, Beijing Yanshan Hotel



Abstract

Liquid crystals (LCs) represent a fascinating state of matter which combines order and mobility on a molecular and supermolecular level. The unique combination of order and mobility results in that LC is typically “soft” and responds easily to external stimuli. The responsive nature and diversity of LCs provide tremendous opportunities as well as challenges for insights in fundamental science, and open the door to various applications. Conventional nematic LCs have become the quintessential materials of LC displays. With the LC displays ubiquitous in our daily life and annual more than \$100 billion market, the research and development of LCs are moving rapidly beyond display applications and evolving into entirely new and fascinating scientific frontiers. In my talk, I will focus on our research and development on self-organized liquid crystalline nanostructures: from energy-saving devices to organic photovoltaics.

Oral Sessions

Oral Session I

Session Chair: Prof. Victor Puchkov, Institute of Geology Ufimian Scientific Centre

Peony Room (牡丹厅), 2nd floor

Saturday, June 14

ID	Paper Title	Speaker	Affiliation	Time
40028	A Laboratory Study of the Effect of CO ₂ /Brine/Rock Interaction on Saturation Exponent of Carbonate Rocks During CO ₂ Sequestration	Abdulrauf Adebayo	King Fahd University of Petroleum & Minerals	13:30-18:30
40062	Hydro-geophysical Investigation of Contaminant Distribution at a Closed Landfill in Southwestern Ontario, Canada	Jianwen Yang	University of Windsor	13:30-18:30
40111	The new Data on Stratigraphy of the Riphean Stratotype in the Southern Urals, Russia	Victor Puchkov	Institute of Geology Ufimian Scientific Centre	13:30-18:30
40133	A Statistical Model for Long-Term Forecasts of Strong Sand Dust Storms	Siqi Tan	Covance Pharmaceutical Research & Development Co.	13:30-18:30
40178	A drilling data-aided seismic mapping method for intermediate-mafic volcanic facies and its application in hydrocarbon exploration	feng yuhui	Jilin University	13:30-18:30
40215	Application of Audio-Magnetotelluric Method for Exploration the Concealed Ore-Bodies in Yuele Lead-Zinc Ore Field, Dagan County, NE Yunnan Province, China	Chuandong Xue	Kunming University of Science and Technology	13:30-18:30
40217	Magnetic Method Surveying and Its Application for the Concealed Ore-bodies Prospecting of Laba Porphyry Molybdenum Ore Field in Shangri-la, Northwestern Yunnan Province, China	Nguyen Ba Dai	Kunming University of Science and Technology	13:30-18:30
40236	Research on Determination of the Main Factors Influencing the Gas Well Post-frac Productivity Prediction for Tight Sandstone Reservoirs Based on Factors Analysis	Jiang Bici	Jilin University	13:30-18:30
40260	Global Warming Impacts on Alpine Vegetation Dynamic in Qinghai-Tibet Plateau of China	Yan Qing Zhang	Simon Fraser University	13:30-18:30

40271	Diabase development characteristics of Eastern Depression of Liaohe Basin and its relationship with fracture	Ang Sun	Jilin University	13:30-18:30
40300	Ophiolite belts of the Taimyr peninsula	Alina Proskurnina	VSEGEI	13:30-18:30
40340	Natalka Gold Deposit	Elena Nikitenko	NEISRI FEB RAS	13:30-18:30
40352	Anaerobic digestion of olive oil mill wastewater pre-treated with catalytic wet peroxide photo-oxidation using copper supported pillared clay catalysts	rym BEN ACHMA	Laboratoire de Chimie des Matériaux et Catalyse	13:30-18:30
40357	Planktonic foraminifera diversity in the Sea of Okhotsk and correlation to past climate change	Alexandra Romanova	Far East Geological Institute	13:30-18:30
40362	Diatoms from Middle Miocene continental deposits of Primorye	Olesya Likhacheva	Far East Geological Institute FEB RAS, Vladivostok	13:30-18:30
40257	Porosity Calculation of Tight Sand Gas Reservoirs with GA-CM Hybrid Optimization Log Interpretation Method	Ya-nan DUAN	Jilin University	13:30-18:30
40369	Geochemistry and Petrography of Alkaline rocks from Monte Santo Alkaline Intrusive Suite, Western Araguaia Belt, Tocantins State, Brazil	Rubia Ribeiro Viana	Federal University of Mato Grosso	13:30-18:30
40047	Viscosity of kimberlite and basaltic magmas at the origin, ascent and eruption	Eduard Persikov	Institute of Experimental Mineralogy RAS	13:30-18:30
40012	Fractal Analysis of Dykes of the Satpura Gondwana Basin, Central India	Chandan Chakraborty	Indian Statistical Institute	13:30-18:30
40348	Some mass migration underground found in Beijing Area	Jinsong Ping	National Astronomical Observatories, CAS	13:30-18:30
40174	A promising way of resource utilization in china: converting waste oils and fats to biodiesel	Shitao Liu	Kunshan Innovation Institute of Nanjing University	13:30-18:30
40359	The design of stall-regulated wind turbine blade for a maximum annual energy output and minimum cost of energy based on a specific wind statistic	WIKANDA SRIDECH	Suranaree University of Technology	13:30-18:30
40264	Optimization of Anaerobic Digestion Process to Obtain Biogas from Date Palm Tree Wastes	Siddig H. Hamad	King Saud University, Saudi Arabia	13:30-18:30
40361	Enhancements of Roof Solar Chimney Performance for Building Ventilation	PORNSAWAN TONGBAI	Suranaree University of Technology	13:30-18:30

Oral Session II

Session Chair: Prof. Michael Kimberley, Princeton University

Plum Blossom Room (沁梅厅), 2nd floor

Saturday, June 14

ID	Paper Title	Speaker	Affiliation	Time
40071	Seismic Structure of The European Crust and Upper Mantle Based on Adjoint Tomography	Hejun Zhu	UT Austin	13:30-18:30
40094	A Generalized Optimal 17-point Scheme for Frequency-domain Scalar Wave Equation	Xiangde Tang	Chinese Academy of Sciences	13:30-18:30
40096	Late Cretaceous Sub-Marine Fan System in Batain Melange Zone, Fayah Formation in South Oman	Iftikhar A. Abbasi	Sultan Qaboos University	13:30-18:30
40099	Well site selection of SK-Iie, Series ICDP Project in Songliao Basin	Xuejiao Qu	Jilin University	13:30-18:30
40108	Geological and geophysical characterization of mafic volcanic reservoirs: an example from eastern sag of Liaoh Basin	Wang Yanquan	Jilin University	13:30-18:30
40109	Element Geochemistry and Tectonic Setting of Greenschists in Central Range of Taiwan	You Long	Jilin University	13:30-18:30
40131	Disastrous Flooding by the Yellow River Cannot be Prevented	Michael Kimberley	Princeton University	13:30-18:30
40132	Correlation among Global Climate Change, Yellow River Flooding, and Dynasty Collapse	Kunhao Li	Princeton University	13:30-18:30
40333	New data on trace element geochemistry of the Gaussberg leucitites (West Antarctica)	Natalya Migdisova	Vernadsky Institute for Geochemistry	13:30-18:30
40334	Interpretational Applications of Spectral Decomposition in Diabase Fractures Prediction	Qiao Wang	Jilin University	13:30-18:30
40317	Flood Risk for Embanked Rivers	Ewa Bogdanowicz	Institute of Meteorology and Water Management	13:30-18:30
40318	On Return Period of the Largest Historical Flood	Witold G. Strupczewski	Institute of Geophysics Polish Academy of Sciences	13:30-18:30
40324	A Study of Sediments and Radioactive Particles of the Yenisei River Using a Variety of Analytical Methods	Alexander Bolsunovsky	Institute of Biophysics SB Russian Academy of Sci	13:30-18:30
40055	Depositional and tectonic constraints for hydrocarbon targets of the Lutetian–Langhian sequences from the Gulf of Gabes — Tunisia	Fatma TAKATK	King Saud University	13:30-18:30

40091	Low-frequency modulation and trend of the relationship between ENSO and precipitation along the Northern to Center Peruvian Pacific coast.	Pedro Rau	GET, Universittade	13:30-18:30
40114	The influence of water area on local climate by using COSMO NWP model	Kristyna Bartunkova	Institute of Atmospheric Physics, ASCR	13:30-18:30
40148	The METRo-CZ model for nowcasting of road surface temperature	Zbynek Sokol	Institute of Atmospheric Physics ASCR	13:30-18:30
40172	The Influence of El Nino on MJO over the Equatorial Pacific	Xiong Chen	PLA University of Science and Technology	13:30-18:30
40197	Aggregation methods in flood frequency analysis	Iwona KuptelMarkiewicz	Institute of Geophysics Polish Academy of Sciences	13:30-18:30
40294	On the Application of Probabilistic Hydrometeorological Simulation of Soil Moisture Across Different Stations in India	Sarit Kumar Das	Indian Institute of Technology, Kharagpur	13:30-18:30
40364	Tsunami Simulation of the April 01, 2014 Chile Earthquake due to Preliminary Results of Point Source and Finite-Fault Source Models	Ergin Ulutas	Kocaeli University, Department of Geophysics	13:30-18:30
40368	SHRIMP U-Pb and U-Pb laser ablation geochronological on zircons from Monte Santo Alkaline Intrusive Suite, Western Araguaia Belt, Tocantins State, Brazil	Rubia Ribeiro Viana	Federal University of Mato Grosso	13:30-18:30

The 2nd Genetics and Genomics Conference (GC 2014) & the 2nd

Int'l Conf. on Biomedical Engineering (ICBE 2014)

Schedule

Registration (June 13-15, 2014)

Location: Lobby, Beijing Yanshan Hotel

Time: June 13, 14:00 - 17:00

Location: 2nd floor, Beijing Yanshan Hotel

Time: June 14, 08:30 - 12:00

Oral Session (June 14, 2014)

Location: Peony Room (牡丹厅), 2nd floor, Beijing Yanshan Hotel

Time: 08:30-12:00 (Coffee Break 10:30-10:45)

Lunch

Location: VISTA CAFÉ (雅景咖啡厅), 1st Floor, Beijing Yanshan Hotel

Time: June 14, 12:00-13:30

Dinner

Location: VISTA CAFÉ (雅景咖啡厅), 1st Floor, Beijing Yanshan Hotel

Time: June 14, 18:30-19:30

One-day Tour (at own expense)

Location: The Great Wall and Ming Tombs (Thirteen Tombs of Ming Dynasty)

Time: June 15, 2014

Oral Session

Session Chair: Prof. Nikolajs Sjakste, Latvian Institute of Organic Synthesis

Peony Room (牡丹厅), 2nd floor

Saturday, June 14

ID	Paper Title	Speaker	Affiliation	Time
40101	Genetic diversity of the PSMA6, PSMC6 and PSMA3 proteasomal genes in Latvian, Lithuanian and Taiwanese populations	Tatjana Sjakste	University of Latvia	08:30-12:00
40112	In Vitro Studies Of 1,4-Dihydropyridine Peroxynitrite Scavenging and Dna Protective Activities	Nikolajs Sjakste	Latvian Institute of Organic Synthesis	08:30-12:00
40033	A novel genetic method for generation of antioxidant mice with graded gene expression	Xianwen Yi	Xinxiang Medical University	08:30-12:00
40184	KeyGene's Green Gene Revolution: molecular mutagenesis for plant breeding	Michiel van Eijk	KeyGene	08:30-12:00
40168	Evaluation of Nasal Functions While Wearing N95 Respirator and Surgical Facemask	Jian Hua Zhu	Dept. ME National University of Singapore	08:30-12:00
40173	Attention Drawing of Movie Trailers Revealed by Electroencephography Using Sample Entropy	Po-Shan Wang	Taipei Municipal Gan-Dau Hospital	08:30-12:00
40176	Data Classification with Modified Density Weighted Distance Measure for Diffusion Maps	Yu-Te Wu	National Yang-Ming University	08:30-12:00
40336	Age-Related Changes in Probability Density Function of Pairwise Euclidean Distances between Multichannel Human EEG Signals	Mikhail Trifonov	IEPB of the Russian Academy of Science	08:30-12:00
40370	Research on thermal effect of electrosurgery with anti-adhesion composite films	Han-Yi Cheng	Biomedical Materials and Tissue Engineering	08:30-12:00
40083	A preliminary phantom study for post-reconstruction material separation using dual-energy micro-computed tomography	Hsiang-Ling Huang	National Yang-Ming University	08:30-12:00
40134	Multimodality Molecular Imaging for Targeted Biopsy of Prostate Cancer	Baowei Fei	Emory University / Georgia Institute of Technology	08:30-12:00
40117	Validation of an Intracranial Aneurysm Image Segmentation Method via use of Silicone Models	SEN yuka	Macquarie University	08:30-12:00
40003	Linkage Study of Autosomal Recessive Nonsyndromic Primary Microcephaly in	Saba Irshad	Punjab University	08:30-12:00

	Pakistani Kindered				
40281	DNA methylation patterns and expression of DNMT1 in rheumatoid arthritis	Attya Bhatti	Atta-ur Rahman	School of Applied Biosciences, Nation	08:30-12:00

Appendix

2014 International Conference on Enzyme (ICE 2014)

Oral Session

Article ID: 40372

Title: Decolorization and Preliminary analyte profiling of synthetic, organic, model, textile dyes using crude fungal laccase from *Rigidoporus* sp. cultivated with wheat bran as solid agro support medium

Name: Suresh P.K.

Affiliation: VIT UNIVERSITY

E-mail: p.k.suresh@vit.ac.in

Abstract

Extracellular crude laccase were produced by *Rigidoporus* sp. by solid substrate fermentation (SSF) using wheat bran as a solid support. Process parameters that influence the decolorization/degradation parameters such as pH, dye concentration (mg/L) and incubation time were investigated. The metabolites formed subsequent to the process of decolorization/degradation were analyzed using UV-VIS, HPLC, LC-MS (Electron Spray Ionization with a Atomic Pressure Chemical Ionization (ESI+APCI) in a negative mode) and Raman spectroscope. Collating the analytical data helps us to understand the biotransformation process. Biotransformation of three textile dyes such as Drimaren Blue HF-RL (HFRL), Acid Blue 113 (AB113) and Reactive Blue 19 (RB19) showed promising results with decolorizability of 64.81%, 97.10% and 30.67% in 60 minutes at their optimum pH (results are the mean values of experiments done in triplicate). The pH optima, under static conditions at room temperature and without the addition of any externally added redox mediators, was 5 (AB113 and HFRL) and pH3 (RB19) respectively. HFRL was rapidly decolorized, with a concomitant decrease in

the absorbance at its absorption maximum. In the case of AB113, absorbance decreased initially within the first 30 minutes, but became saturated after one hour of incubation, leading to a darkening of the reaction mixture, probably due to the formation of polymerization reaction among the products, breakdown products and the dye producing soluble polymers. RB19 reported a decrease in the absorbance within one hour of incubation. This preliminary metabolite profiling provides some insights and possibly a better understanding of the degradation process, specifically mediated by a crude laccase from *Rigidoporus* sp., apart from validating the potential of our approach for bioremediation of textile dye effluents.

Article ID: 40314

Title: Oral Submucous Fibrosis - Genetic Aspects of the Mechanistically-linked Enzymes and those associated with pathogenesis of this pre-malignant, fibrotic condition of the Oral Cavity

Name: Suresh P.K.

Affiliation: VIT UNIVERSITY

E-mail: p.k.suresh@vit.ac.in

Abstract

Oral Submucous Fibrosis (OSF) is a pre-malignant, pathological, fibrotic condition of the oral cavity affecting people of Asian/South East Asian descent^{1,2}, involving TGF- β . The principal causative agent is areca nut in its processed and non-processed forms³. Despite Governmental bans on the sale of this product in India, its use is continuing and has reached epidemic proportions, especially due to its easy accessibility, social acceptability and addictive potential and is associated with oral mucosal disorders including OSF^{4,5}. There are wide geographic

variations in the type and form of product chewed⁶. However, not all chewers are afflicted with this condition, thereby implying a genetic predisposition to those afflicted with OSF⁷, apart from the role of slaked lime and inflammation⁸. The presence of palpable fibrous bands (alterations in fibro-elastic properties)⁹ as well as the inter-incisor distance (decrease in mouth-opening ability–trismus) has been used by the dentist/oral health specialist as diagnostic criteria with the gold-standard method continuing to be immuno-histochemical localization of antigens following an invasive biopsy¹⁰. There are a number of treatment modalities including chemotherapy (synthetic and ethno-based) as well as surgery¹¹. However, there is currently no cure and the mechanistic details in terms of the pathogenesis are not entirely clear¹². OSF is known to be due to disturbances in the equilibrium between collagen synthesis (for e.g., Col 1A1, Col 1A2) and breakdown (for e.g., Collagenase-1). Hence, variations in the genes encoding for enzymes involved in the synthesis and breakdown may result in alterations in activity and hence alter the risk profile of that individual in terms of his/her susceptibility to acquiring this areca nut-mediated condition. Also, variations in the activity of lysyl oxidase – a major enzyme involved in cross-linking and maturation of collagen may also serve to flag individuals at risk by possibly stabilizing collagen and decreasing its degradation^{13,14,15}. Further, allelic variants of Glutathione-S-Transferases (GSTs) (polymorphic enzymes), can affect the activity of the enzyme and can increase the susceptibility of the host for this condition. Specifically, it has been reported that the presence of the null genotype (GSTM1 and GSTT1), singly or in combination, can increase the risk for OSF in comparison with the controls, and can be considered an associative marker^{16,17}. There are reports documenting epigenetic changes in key genes like E-cadherin and Cyclo-oxygenase-2 (COX-2) being correlated with OSF, in comparison with Oral Cancer¹⁸. There has been only one study globally, performed by a Taiwanese group, relating polymorphisms in collagen-related genes (for e.g., Collagenase-1

(COLase), Lysyl Oxidase) (LYOXase), and cystatin C (CST3)) and OSF (correlated to nut-years) in comparison with hospital and community-based controls¹⁹. Hence, there is an unmet need to perform well-designed case-control studies in Indian populations, specifically cataloging all the relevant allelic variants in collagen-metabolism-related enzymes as well as those contributing to the alterations in susceptibility to this condition in different ethnic populations²⁰. This can eventually lead to the development of an OSF-specific haplotype²¹ to complement the efforts to develop transcriptomic and proteomic signatures specifically for OSF, apart from the possibility of identifying/validating key biomarker(s). like MMP-1, TIMP-1/2 that can be of diagnostic and/or prognostic relevance^{22,23}. This aspect should be seen in the context of the increasing public health burden due to this areca nut-induced condition, despite the increasing awareness of the harmful effects of this 4th psychoactive substance after caffeine, nicotine and alcohol²⁴.

Article ID: 40282

Title: Studies on xyloglucanase during the germination of seeds of *Tamarindus indica*

Name: SiddalingaMurthy Kora Rudraiah

Affiliation: BANGALORE UNIVERSITY

E-mail: krsmurthy2001@yahoo.com

Abstract

Germinating seeds of *Tamarindus indica* contain endo- β -1, 4-xyloglucanases which degrade tamarind xyloglucan, but not carboxymethylcellulose (CMC). The xyloglucanases are isolated from the germinating tamarind seeds using 50 mM acetate buffer, pH 5.5 containing 0.5 M NaCl. The Km value is 0.667 g / liter and the enzyme is optimally active at pH 5.5 and stable between pH 4 – 6.5. The optimum temperature is 45° C and is quite stable upto 50° C. The activity declined by 50 % at 60° C and is completely inactivated at 70° C. Highest xyloglucanase activity and specific activity are observed on the 23rd day of

germination. The polyacrylamide gel electrophoresis (PAGE) indicated the presence of five isozymes of xyloglucanases which are visualized by activity staining separately with congo red and grams iodine. Isozyme 2 is the major xyloglucanase present throughout the germination period.

Article ID: 40363

Title: Characterization of esterases of Tamarindus indica seeds

Name: KANTHARAJU S

Affiliation: BANGALORE UNIVERSITY

E-mail: kantharaj2553@gmail.com

Abstract

Germinating seeds of Tamarindus indica synthesizes various enzymes which are required for the degradation of seed reserves such as xyloglucans, fatty acid esters and proteins. Among these, esterases, belonging to a group of hydrolytic enzymes catalyze the hydrolysis of various types of esters. They play an important role in cell expansion as well as detoxification of xenobiotics and many agrochemicals and insecticides. The esterases are extracted from the germinating tamarind seeds using 50 mM phosphate buffer, pH 7. The K_m with α -naphthyl acetate as the substrate is 19.23 μ M and the enzymes are optimally active at pH 7.0 to 7.5 and are stable between pH 5.0 to 9.0. The optimum temperature of esterase activity of tamarind seed is between 37 – 50° C and is stable up to 40° C. The activity declined by 30 % at 60° C and about 90 % at 70° C. Highest esterase activity and specific activity are observed on the 21st day of germination. The polyacrylamide gel electrophoresis (PAGE) indicated the presence of nine isozymes of esterases. Band numbers 1, 5 and 6 are the major esterolytic bands present throughout the germination period while band numbers 2 & 3 are minor bands present only during the latter period of the germination. Based on substrate and inhibitor specificity in conjunction with electrophoresis, the esterases 1 to 8 have been classified as carboxylesterases sensitive to organophosphate

inhibitor (OP) and PCMB (p-chloromercuribenzoate) while esterase 9 is classified as carboxylesterase sensitive to OP. These esterases are unaffected by carbamate inhibitor, eserine sulphate.

Article ID: 40284

Title: Enzyme kinetic equations of irreversible and reversible reactions in metabolism

Name: Josep J. Centelles

Affiliation: Universitat de Barcelona

E-mail: josepcentelles@ub.edu

Abstract

This paper compares the irreversible and reversible rate equations from several uni-uni kinetic mechanisms (Michaelis-Menten, Hill and Adair equations) and bi-bi mechanisms (single- and double-displacement equations). In reversible reactions, Haldane relationship is considered to be identical for all mechanisms considered and reversible equations can be also obtained from this relationship. Some reversible reactions of the metabolism are also presented, with their equilibrium constant.

Article ID: 40295

Title: Catalytically important residues in E. coli 1-deoxy-D-xylulose 5-phosphate synthase

Name: Santiago Imperial

Affiliation: Universitat de Barcelona

E-mail: simperial@ub.edu

Abstract

1-deoxy-D-xylulose 5-phosphate synthase (DXS) catalyzes the initial step of the 2-C-methyl-D-erythritol 4-phosphate (MEP) pathway consisting in the condensation of (hydroxyethyl)thiamin derived from pyruvate with D-glyceraldehyde 3-phosphate (GAP) to yield 1-deoxy-D-xylulose 5-phosphate (DXP). The role of the conserved residues H49, E370, D427 and H431 of E. coli DXS was examined by site-directed mutagenesis and kinetic analysis of the purified

recombinant enzyme mutants. Mutants at position H49 showed a severe reduction in their specific activities with a decrease of the k_{cat}/K_M ratio by two orders of magnitude lower than the wild-type DXS. According to available structural data residue H49 is perfectly positioned to abstract a proton from the donor substrate. Mutations in DXS E370 showed that this residue is also essential for catalytic activity. Three-dimensional structure supports its involvement in cofactor deprotonation, the first step in enzymatic thiamin catalysis. Results obtained with H431 mutant enzymes indicate that this residue play a role contributing to transition state stabilization. Finally, mutants at position D427 also showed a severe specific activity decrease with a reduction of the k_{cat}/K_M ratio. A role in binding the substrate and selecting the stereoisomer is proposed for this residue.

Article ID: 40151

Title: Non-classical cytochromes P450 of the CYP74 family

Name: Svetlana Gorina

Affiliation: Kazan Institute of Biochemistry and Biophysics

E-mail: gsvetlana87@gmail.com

Abstract

Divinyl ether synthases (DESs) are members of the CYP74 family of cytochromes P450 that are specialized for the metabolism of fatty acid hydroperoxides along with allene oxide synthases (AOS) and hydroperoxide lyases (HPL). In contrast to classical P450 monooxygenases the CYP74 enzymes does not require molecular oxygen neither redox partner for their catalytic activities. The new carbon-oxygen bonds are formed as a result of conversion of acyl hydroperoxide which is both the substrate and the oxygen donor. AOSs and HPLs are widespread in plant kingdom, where as DES activities have been detected in limited number of plant species from absolutely different taxons. Until recently only five DES genes were cloned and corresponding recombinant enzymes were characterized. Four of

them are strictly 9-specific enzymes of closely related Solanaceae species and the fifth DES is 9/13-specific enzyme from garlic. So researchers suggested that 9-specificity is typical for DESs. However, a number of divinyl ethers produced from 13-hydroperoxides have been detected in different plant species. Unfortunately, absence of genome data impedes detection of novel genes. In 2010 we solved this problem when constructing the system of universal degenerated primers for CYP74s searching. This system allowed us to clone the first 13-hydroperoxide-specific divinyl ether synthases from flax (*Linum usitatissimum* L.) (LuDES), buttercup (*Ranunculus acris* L.) (RaDES) and Lycopodiophyta (*Selaginella moellendorffii*) (SmCYP74M3). These enzymes effectively metabolized 13-hydroperoxides of α -linolenic (13-HPOT) and linoleic acids (13-HPOD), but are not active against the corresponding 9-hydroperoxides. The preferred substrate for LuDES and RaDES were the 13-hydroperoxide of α -linolenic acid, and the reaction product was identified by mass spectrometry, NMR and UV spectroscopy as the divinyl ether – (omega5Z)-etherolenic acid. Incubations of (13S)-HPOD with SmCYP74M3 enzyme afforded several different divinyl ethers (isolated as its methyl esters). Their structures were also identified by mass spectrometry, NMR and UV spectroscopy. Detection of 13-DESs complements the common scheme of the CYP74 catalysis and confirms our hypothesis of the CYP74 clan origin and evolutionary history of P450 superfamily. This work is partly supported by Russian Foundation of Basic Research (13-04-40103-H, 14-04-01532, 12-04-97087-r, 12-04-97059-r), MK-4886.2013.4 and SS-1890.2014.4.

Article ID: 40154

Title: Unusual cytochrome P450 of brown alga *Ectocarpus siliculosus*

Name: Valeriia Ermilova

Affiliation: Kazan Institute of Biochemistry and Biophysics

E-mail: ntdes@mail.ru

Abstract

Cytochromes P450 – haem-thiolate enzymes common for all eukaryotic organisms. This superfamily consists of hundreds families and several clans. The most unusual enzymes among cytochromes P450 belong to the CYP74 clan. Almost all cytochromes P450 are monooxygenases and they metabolize two substrates: oxidized compound and molecular oxygen. Unlike the monooxygenases, the CYP74 enzymes have an atypical reaction mechanism that requires neither oxygen nor an NADPH-reductase. Therefore their substrate recognizing sites and domains forming active center differ from those of classic P450s. For example, there is no oxygen-binding domain in the CYP74s structure. Like in all P450s the fifth ligand of haem is cysteine but haem-binding loop is not the same to that of classical monooxygenase. The CYP74 enzymes have insertion of 9 amino acid residues before the cysteine that makes the loop to be closer to the surface of the protein molecule. The CYP74 clan includes hydroperoxide lyases (HPLs), allene oxide synthases (AOSs), divinyl ether synthases (DESS) and the most poorly studied epoxy alcohol synthases (EASs). Despite differences in product specificities, they all metabolize 9- and/or 13-hydroperoxides as substrates, which are produced by the oxygenation of polyunsaturated fatty acids by the action of lipoxygenases (LOX). The CYP74 clan members have been found in a wide variety of organisms including animals, plants, bacteria but not algae. Despite this fact oxylipins were detected in different algae species. Analysis of data base containing genome of brown algae *Ectocarpus siliculosus* with open reading frames revealed 12 sequences which have high homology with cytochromes P450 of higher plants. One of these sequences has similarity with the CYP74 enzymes. We obtained corresponding recombinant protein using *E. coli* expression system. Affinity-purified protein EsCYP74 was incubating with model substrates – 9- and 13-hydroperoxides of linoleic acid. As a result of incubation there was detected a range of epoxy alcohols and dihydroxy

acids. The structures of all products have been resolved using GC-MS and NMR. Thus, the described enzyme is the first member of the CYP74 clan detected in algae, and it belongs to one of the most poorly studied groups of the CYP74 enzymes – epoxy alcohol synthase. Detection of the CYP74 enzyme in algae complements the common scheme of the CYP74 catalysis and confirms our hypothesis of the CYP74 clan origin and evolutionary history of P450 superfamily. This work is partly supported by Russian Foundation of Basic Research (13-04-40103-H, 14-04-01532, 12-04-97087-r, 12-04-97059-r), MK-4886.2013.4 and SS-1890.2014.4.

Article ID: 40155

Title: Alterations of the catalytic mechanisms of unusual cytochromes P450 as a result of site-directed mutagenesis

Name: Yana Toporkova

Affiliation: Kazan Institute of Biochemistry and Biophysics

E-mail: yanchens@yandex.ru

Abstract

Unlike most of the cytochromes P450 which are monooxygenases, enzymes of the CYP74 family do not require molecular oxygen nor NAD(P)H-dependent cytochrome P450 reductases as cofactors, but use their hydroperoxide substrates as source for reducing equivalents and as oxygen donor. So their oxygen-binding domain is degenerate and substituted by I-helix central domain (IHCD) which participates in the CYP74 catalytic action. The CYP74 enzymes converse their fatty acid hydroperoxide substrates into various structurally different products: allene oxide synthases (AOSs) catalyze the formation of short-lived allene oxides which hydrolyze into ketols or cyclize into cyclopentenones; divinyl ether synthases (DESS) convert hydroperoxides to divinyl ethers, and hydroperoxide lyases (HPLs) produce short-lived hemiacetals that decompose to aldehydes and α -fatty acids. Thus, AOSs and DESS function as

dehydrases, and HPLs are isomerases. Alignment of the CYP74s primary structures revealed several conservative domains; some of them fall into substrate-recognition sites (SRSs) which are typical for all P450s. Number of sites within these domains were chosen, and amino acids at those sites were substituted. The obtained data demonstrate the interconversions of the CYP74 enzymes as a result of site-directed mutagenesis. Two mutations led to complete conversions: AOS into HPL and DES into AOS. Some more mutations led to alterations of the CYP74s catalytic activities in different ratios: from partial to almost complete. Moreover, several mutants with dual and trial activities were obtained. On the other hand, no one case of the CYP74s regiospecificity change caused by site-directed mutagenesis was detected. Thus, the results of site-directed mutagenesis revealed primary determinants of the CYP74 catalysis. The data demonstrate that the catalytic mechanisms of the CYP74 enzymes are closely related. The results of site-directed mutagenesis indicate that the epoxyallylic radical is the switching point of the CYP74 catalysis. Depending on primary sequence of the conservative domains, the epoxyallylic radical either undergoes the rearrangement into the vinyl ether radical, which is then recombined with hydroxyl radical to afford the hemiacetal (HPL pathway), or undergoes the deprotonation to form the allene oxide (AOS pathway), or undergoes the homolytic opening of oxirane to form the vinyl ether carbonyl radical which loses a hydrogen atom to afford divinyl ether (DES pathway). This work is partly supported by Russian Foundation of Basic Research (13-04-40103-H, 14-04-01532, 12-04-97087-r, 12-04-97059-r), MK-4886.2013.4 and SS-1890.2014.4.

Article ID: 40381

Title: New enzymatic reaction for the synthesis of a carbon-nitrogen bond

Name: Michihiko Kobayashi

Affiliation: University of Tsukuba

E-mail: kobay@agbi.tsukuba.ac.jp

Abstract

Pseudomonas chlororaphis B23 strain is able to grow on the medium containing nitrile (R-CN) as the sole carbon and nitrogen sources. We clarified the nitrile hydratase (NHase) gene cluster, which consists of seven genes (i.e. *oxdA*, *amiA*, *nhpA*, *nhpB*, *nhpC*, *nhpS* and *acsA*); e.g. *OxDa* is aldoxime dehydratase; *AmiA* is amidase; *NhpA* is NHase alpha-subunit; *NhpB* is NHase beta-subunit; *AcsA* is acyl-CoA synthetase)[1-3]. We also clarified the regulation mechanism of their gene expression. Through the investigation of the culture condition, RT-PCR and gene disruption experiments, we found *acsA* encodes acyl-CoA synthetase (*AcsA*), and plays an essential role in acid utilization in the nitrile-degradative pathway [4]. *AcsA* ligates acid with CoA to form acyl-CoA with a carbon-sulfur bond. However, when L-cysteine was used as a substrate instead of CoA, N-acyl-L-cysteine was surprisingly detected as a reaction product. This finding demonstrates that *AcsA* synthesizes an amide bond comprising the amino group of cysteine and the carboxyl group of the acid. *AcsA* formed a variety of N-acyl-compounds, when various acids and cysteine-analogues were used as substrates. Enzymes of the adenylate-forming enzyme superfamily, which *AcsA* belongs to, were also found to catalyze the similar reaction. Furthermore, we discovered that adenylation domains of nonribosomal peptide synthetases, which belong to the same superfamily showed the peptide-bond synthetic activity. Various dipeptides can be synthesized by the adenylation domains.

Article ID: 40331

Title: Thermostable S-adenosylhomocysteine hydrolase from *Thermotoga maritima*: Properties and its application on S-adenosylhomocysteine production with a cofactor regeneration system

Name: Guojun Qian

Affiliation: Nanjing Normal University

E-mail: qianguojun0609@gmail.com

Abstract

S-Adenosylhomocysteine hydrolase (SAHase) catalyzes the reversible conversion of adenosine and homocysteine to S-Adenosylhomocysteine (SAH). SAH is an effective sedative, a good sleep modulator, and a new potential anticonvulsant. The extremely thermostable SAHase and lactate dehydrogenase (LDH) from *Thermotoga maritima* were overexpressed in *Escherichia coli* and easily purified to gel electrophoretic homogeneity. The SAHase exhibited highest enzymatic activity at 85°C and pH 8.0 with a specific activity of 6.2 U/mg at 1 mM NAD. Under these conditions, 24 μmol SAH was obtained when 0.5 mg SAHase was applied to a 10-ml reaction mixture; SAH production was further increased to 153 μmol by adding LDH and its substrate into the reaction mixture. Therefore, extremely thermostable enzymes SAHase and LDH form an efficient NAD consumption and regeneration system for SAH biosynthesis at elevated temperatures. This is the first report for the production of SAH from adenosine and homocysteine by coupling an efficient cofactor regeneration system.

Article ID: 40358

Title: A Feasibility Study on Production and Application of Thermostable Laccase and Xylanase in Pulp Biobleaching

Name: Hongcheng Wang

Affiliation: Biofuels Institute, Jiangsu University

E-mail: hcwang2870@163.com

Abstract

Enzymatic delignification of pulp provides an environment-friendly bleaching strategy. However, the costs of the enzymes to be used for biobleaching need to be reduced, and the enzyme activities should be increased to make the process feasible. Thermostable laccase and xylanase have advantages in their higher reaction rates and longer life time at the elevated temperatures occurring in pulp-bleaching process. Thermostable laccase gene of *Thermus thermophilus* and xylanase B gene of *Thermotoga maritima* were

cloned and overexpressed in *Escherichia coli*. In gene expression system pHsh, the expression of target gene is under control of an alternative Sigma factor, Sigma 32 of *E. coli*, which not only eliminates the cost for a chemical inducer such as IPTG, but also activates chaperon expression and allows host cells to grow to high densities. By using pHsh vectors, the expression levels of thermostable laccase and xylanase reached 52% and 32% of total soluble protein of *E. coli*. The recombinant laccase and xylanase were easily purified by a step of heat treatment and applied to biobleaching tests over wheat straw pulp. The optimal biobleaching process includes treating 10% wheat straw pulp at 85°C, pH 4.8 for 120 min with 10 U xylanase or 5 U laccase per gram of dry pulp. Compared with conventional straw pulp bleaching process, the treatment of thermostable laccase or xylanase can reduce the use of sodium hydroxide and the produce of alkaline wast water in pulp bleaching process, save over 25% of hydrogen peroxide or chlorine dioxide, and increase the strength of paper as well. The combination of the laccase and xylanase gave higher brightness of wheat straw pulp. Therefore, the enzymatic delignification of pulp by using thermostable laccase and xylanase can be economically beneficial to paper industry.

Article ID: 40355

Title: Prospective clinical application of thioredoxin reductase as a novel diagnostic tumor marker

Name: Aaron Yep

Affiliation: Health Science Center, Peking University

E-mail: pkuyesuofu@163.com

Abstract

Developing a novel, efficient biomarker for detecting malignant tumors is essential for the early diagnosis of cancers. Our aim was to assess the diagnostic value of a potential plasma tumor marker, thioredoxin reductase (TR), which is expressed in many types of malignant tumor, for the non-invasive detection of cancers. Methods: The plasma activities of TR were measured in 1,513 patients with common clinical diseases, 59 patients with benign tumors, and 154

patients with cancers and 586 healthy controls. The area under the ROC curve (AUC) of TR and logistic regression results of different groups were compared by sensitivity, specificity and Youden's index. Diagnostic cut-offs and clinical reference intervals were established via ROC curve analysis. Results: The logistic regression indicated that TR activity can discriminate between cancers and benign tumors or other common diseases very well ($p < 0.0001$), with an area under the curve from the receiver-operator characteristics between 0.91 and 0.96. The positive critical value was 2.51 and the cancer critical value was 9.90. The diagnostic gray zone (2.51–9.90) may be associated with benign tumors and some common clinical diseases. Conclusions: As a novel potential marker of malignant tumors with quantitative evaluation of proliferation, TR activity detection has an excellent diagnostic potential for early-stage malignant tumors. Impact: The convenient, economical, relatively non-invasive, and reproducible detection method of TR activity makes it suitable for routine clinical practice.

Article ID: 40342

Title: Methodological studies on the detection of thioredoxin reductase activities in laboratory research and clinical trials

Name: Weiwei Ma

Affiliation: Health Science Center, Peking University

E-mail: weiweima_23@163.com

Abstract

Human Trx/TR system is highly relevant to the processes of tumorigenesis. Many previous studies have shown that expressions or activities of Trx/TR system are up-regulated in a variety of tumor cells and pre-neoplastic cells. Here, we investigated the TR activities in plasma of 667 healthy individuals and 309 malignant tumor patients by using Detection Kit (Clairvoyance Health Technology Co., Ltd, Wuhan, China; CFDA: Approval No.3400264-2014). In laboratory research, we study on the parameters of the methodology including the analyses of sensitivity,

accuracy, precision and stability for this detection assay. The Statistics Analysis System 9.1 (SAS 9.1) was used for the statistical analysis of the data. The interquartile range of the data was used to present the plasma TR levels. To further assess the ability of TR activity for cancer prognosis, ROC curves, an area under the curve (AUC), Youden's index and the cut-off values were also calculated to set up the clinical reference intervals. Results: The laboratory research: Sensitivity: the limit of detection (LOD) was 1.20 U/mL; as shown in Figure 1, the linear range was 1.2-60.0 U/mL ($Y = 7.26003 + 123.50208 * X$, $R = 0.98641$) when the concentration of TR standard protein was 0 mg/mL-0.5 mg/mL. Accuracy: the TR activities of negative samples were less than 4.0 U/mL; while of positive samples were more than 30.0 U/mL. The agreement rate of two sample groups both reached at 100%. Precision: the CV within group was 8.11%; the CV between groups was 0%. Stability: under the condition of 37°C, reagents in the TR kit can be stably stored for 7 days. The clinical trials: The interquartile ranges of plasma TR levels indicated that the TR level of the subpopulation in the highest quartile (78.92%) is almost 7.93 times more than those in the lowest quartile (9.95%), which demonstrated the strong correlation between the processes of tumorigenesis and plasma TR activity. Logistic regression showed that plasma TR activity was significantly different between healthy controls and malignant tumor patients ($P < 0.05$). The AUC of plasma TR activity in healthy individuals and malignant tumor patients was 0.836 ± 0.015 ; the cut-off value between two groups was set as 7.1U/mL. According to the ROC curve and the stepwise logistic regression, the sensitivity, specificity and Youden's index of plasma TR activity were 68%, 89%, and 82%, respectively. In conclusion, it is a technically convenient, economically beneficial and scientifically reproducible way to evaluate the abnormal hyperplasia level by detecting plasma TR activity with the Detection Kit for TR Activity, which has been approved by China Food and Drug Administration. TR activity detection can be used as a rapid, accurate and precise method for the diagnosis of early-stage

malignant tumors, which is appropriate for future

routine clinical detection.

2014 International Conference on Catalysis (ICC 2014)

Oral Session I

Article ID: 40086

Title: Highly dispersed Cu-base catalyst derived from layered double hydroxides for CO Hydrogenation

Name: Xinyou Han

Affiliation: Institute of Coal Chemistry, CAS

E-mail: xy_han@live.com

Abstract

Highly dispersed Cu-base catalyst has been prepared via thermal decomposition of layered double hydroxides precursors. The XRD pattern and the HRTEM images of the as prepared catalyst confirmed the high dispersion of Cu and Fe ions. Result show that the catalyst has a relatively high selectivity of alkanes at low temperature.

Article ID: 40115

Title: A Functional Hmd Analogue That Catalyzes Heterolytic Dihydrogen Cleavage and Hydrogenation of Quinone under Mild Condition

Name: Shuang Jiang

Affiliation: Collaborative Innovation Center of Chemical Scienc

E-mail: jstju2007@126.com

Abstract

An unsaturated pentacoordinated mono iron di-carbonyl complex (complex 1, Fe(CO)₂IMes(NS)) with a nitrogen heterocyclic carbene (NHC) ligand and 2-amidothiophenolate dianion bidentate non-innocent ligand was reported in this work as a model of [Fe]-hydrogenase active site. This model complex possesses the same coordinated atoms and similar geometry as the [Fe]-hydrogenase active site and exhibits proton coupled CO binding behavior. The

NHC carbon coordinated trans to an open site as the acyl carbon in [Fe]-hydrogenase active site. Moreover, this complex exhibit H₂ activation and catalytic hydrogenation of quinone to hydroquinone in mild conditions (1atm H₂, 25°C). Inspired by Noyori's metal-ligand bifunctional catalysis mechanism, we introduce quinone as assistance for H₂ cleavage combined with Fe-NH moiety building in the model complex. The six atoms of -Fe-H-C-O-H-N- in our six-membered ring coincide with the transition state proposed by Hall and coworkers. Based on this catalytic hydrogenation reaction related kinetics and proposed mechanism were explored.

Article ID: 40120

Title: Enhanced Photocatalytic Hydrogen Production Rate via Controlling Surface Transition State Geometry on Selectively Exposed Pt Facet on Pt/TiO₂

Name: Gongxuan Lu

Affiliation: lanzhou Institute of Chemical Physics

E-mail: gxlu@lzb.ac.cn

Abstract

We reported the results of the modulation of photogenerated electrons transfer and photocatalytic hydrogen evolution behaviors of Pt/TiO₂ photocatalyst via controlling surface potential energy on selectively exposed Pt facet for a highly efficient photocatalytic hydrogen generation from water. Pt{111}/TiO₂ photocatalyst exhibited higher photocatalytic hydrogen generation activity than Pt{100}/TiO₂ and Pt{100/111}/TiO₂. As evidenced by photoluminescence spectra, and photoelectrochemical characterizations, Pt{111} facet was more effective in trapping electrons from TiO₂ conduction band for its higher Fermi level. Pt{111}/TiO₂ exhibited lower apparent activation

energy than others because it can provide more reaction sites for water reduction. The formation of hydrogen via H-H recombination was more likely to occur on Pt{111} facets because of its reasonable transition state geometry. This study discloses the facet-dependent effect of noble-metal cocatalyst on semiconductors in photocatalytic water reduction, and will give an insight into design of high-efficient metal/semiconductor hybrid photocatalysts.

Article ID: 40136

Title: Preparation of a Carbon-Based Solid Acid with High Acid Density via a novel method

Name: SiYu OuYang

Affiliation: Hunan University

E-mail: xuqiong139@126.com

Abstract

A carbon-based solid acid with high acid density was successfully prepared using camphor tree branches as raw materials through a novel method including dilute sulfuric acid activation, carbonization in refluxing solvent and sulfonation. Physical characterization was detected to show that the carbon-based acid is amorphous with polycyclic aromatic carbon sheets attached plentiful -OH, -COOH, and -SO₃H groups. The sulfonic acid density and total acid density of it reached 2.05 mmol g⁻¹ and 5.63 mmol g⁻¹ respectively, by acid-base titration. As a solid acid catalyst, it showed excellent performance in the ketalization of cyclohexanone with glycol.

Article ID: 40190

Title: Template-free synthesis of Bi₂O₃-Bi₂S₃ composites of novel morphologies and their enhanced photocatalytic properties

Name: Shuang-Feng Yin

Affiliation: Hunan University

E-mail: yinsf73@163.com

Abstract

Fabrication of composite photocatalysts with

heterojunctions has been provided to be a feasible method for the synthesis of highly efficient photocatalysts.[1-4] Bismuth sulfide (Bi₂S₃), as an important V-VI semiconductor material with direct narrow band-gap (1.3-1.7 eV), showed strong absorption in the visible light region ($\lambda \leq 800$ nm). Because of the facile recombination of photogenerated electrons and holes, photocatalytic activity of Bi₂S₃ is limited.[5] However, it is good visible light sensor when combined with other semiconductors.[6] Considering the similar structures between Bi₂O₃ and Bi₂S₃, it was expected to combine Bi₂S₃ on the surface of Bi₂O₃ to form heterojunctions and thus enhance their visible light induced activities. The solubility of Bi₂O₃ and Bi₂S₃ is incommensurable (K_{sp} of Bi₂O₃ and Bi₂S₃ are 4×10^{-31} and 1×10^{-97} , respectively), which promotes us to prepare Bi₂S₃ on the surface of Bi₂O₃ by a corrosion method.

Article ID: 40199

Title: Air-stable organoantimony complexes: Synthesis, characterization and catalysis

Name: Renhua Qiu

Affiliation: Hunan University

E-mail: yinsf73@163.com

Abstract

The air-stable organoantimony fluoride was successfully synthesized via unexpected B-F bond cleavage activated by antimony, and can be used as bifunctional Lewis acidic/basic catalyst in amination of epoxides with high catalytic efficiency, diastereoselectivity, and recyclability.

Article ID: 40268

Title: Hierarchically structured NiO/CeO₂ nanocatalysts templated by eggshell membranes for methane steam reforming

Name: Zhitao Wang

Affiliation: Curtin University

E-mail: zhitao.wang@postgrad.curtin.edu.au

Abstract

A template synthesis process has been studied to prepare hierarchically structured NiO/CeO₂ nanocatalysts by using eggshell membranes as a template. The templated catalyst is constructed by interwoven ceramic fibres, and the fibres have a nanoporous structure with NiO nanoparticles supported on a CeO₂ scaffold. The effects of immersion time and calcination temperature on catalyst microstructure were investigated using SEM, XRD, TGA and TPR techniques. The catalyst prepared with an immersion time of 3 h has a robust structure that is able to resist internal thermal stresses caused by cooling down after calcination. Calcination temperature greatly affected the performance of steam reforming via catalyst microstructure. Both particle size and the interaction between NiO and CeO₂ determined the reforming performance. The catalyst calcined at 950 °C achieved the highest and most stable methane conversion owing to the optimized microstructure. The strong NiO–CeO₂ interaction is critical to achieve coking-resistance. The three-dimensional structure of the fibrous catalyst ensured the high thermal stability of the nanocatalyst in terms of high resistance to catalyst sintering.

Article ID: 40020

Title: Catalytic combustion of acrylonitrile over 3d-transition metals (Cu, Co, Fe) or Pt/SBA-15, Cu/SBA-16 and Cu/KIT-6 mesoporous catalysts

Name: Dongjun Shi

Affiliation: Beijing University of Chemical Technology

E-mail: shidongjun2009@163.com

Abstract

A series of 3d-transition metals (Cu, Co, Fe)/SBA-15, Pt/SBA-15 and Cu/(SBA-16, KIT-6) catalysts were prepared via an impregnation method, and further characterized by XRD, N₂ physical isothermal adsorption, TEM, H₂-TPR and XPS. The as-prepared catalysts were assessed for the catalytic combustion of

acrylonitrile (C₂H₃CN) with O₂. Ordered mesoporous structure of SBA-15, SBA-16 and KIT-6 were well maintained even after impregnating the various metallic components. At 400 °C, the C₂H₃CN conversion of the investigated catalysts followed a trend of Pt/Co ≈ Cu/Fe/SBA-15, whereas the N₂ yield followed the trend of Cu/Fe/Pt/Co/SBA-15. Apart from the target product of N₂, undesired byproducts (NO, NO₂, N₂O, NH₃, and CO) were also observed during the catalytic combustion. Among the prepared samples, Cu/SBA-15 exhibited a nearly complete C₂H₃CN conversion associated with a N₂ selectivity around 64% at T = 400 °C. It was regarded as a promising material for the catalytic removal of C₂H₃CN. Both the redox properties and chemical natures of the loaded metals were verified to be decisive factors for the corresponding activities and selectivities. Moreover, three mesoporous support of SBA-15, SBA-16, and KIT-6 revealed that the straight cylindrical pores with 2-D arrangement of SBA-15 probably produced homogeneous distribution of the loaded copper along the pore surface and the main species of the highly dispersed Cu²⁺ ions over Cu/SBA-15 displayed the higher C₂H₃CN conversion and the excellent N₂ selectivity. As contrast, the combustion of the three nitrile gases (C₂H₃CN, CH₃CN, and HCN) was respectively conducted over Cu/SBA-15, suggesting that the activity and selectivity were simultaneously controlled by the active sites and the molecule structure of reactants. Furthermore, the C₂H₃CN combustion mechanisms by DRIFTS study separately complied with the “N₂ formation” mechanism over Cu/SBA-15 and the “NH₃ formation” mechanism over Fe/SBA-15.

Article ID: 40021

Title: An Economical Way to Synthesize SSZ-13 for an Extraordinary Performance in Selectively Catalytic Reduction (SCR) of NO_x by ammonia

Name: Ruinian Xu

Affiliation: Beijing University of Chemical Technology

E-mail: xrn883612@126.com

Abstract

The removal of nitrogen oxides (NO_x) coming from auto exhausts has drawn more attention in the past decades because NO_x are known to cause lots of environmental problems such as acid rain and photochemical smog in the urban and industrial areas[1]. Series of legislations were established in Europe, United States, and Japan. NO_x containing in the exhausts are expected to be reduced to a very limited level. Owing to these increasingly stringent environmental regulations, it becomes urgent to develop the new techniques aiming at the highly efficient auto-emission purification. SSZ-13 zeolite, a CHA-type aluminosilicate, was verified to be a suitable candidate to develop the promising catalysts for NH₃-SCR of NO reaction[2,3]. However, the conventional method to synthesize the SSZ-13 zeolite involving the use of a very expensive template (N,N,N-trimethyl-1-1-adamantammonium hydroxide)[4]. In this work, an economical way for SSZ-13 preparation was attempted. The as-synthesized SSZ-13 zeolite after ion exchange by copper nitrate solution exhibited a superior SCR performance than the traditional commercial zeolitic catalysts of Cu-Beta and Cu-ZSM-5.

Article ID: 40022

Title: Selective catalytic oxidation (SCO) of ammonia to nitrogen over mesoporous zeolite

Name: Runduo Zhang

Affiliation: Beijing University of Chemical Technology

E-mail: ptformail@gmail.com

Abstract

A wide range of transition metals modified SBA-15 samples (M/SBA-15) [M = 3d transition metals (Cu, Co, Fe, Mn, Ni) and Cu supported on SBA-16, KIT-6] was prepared and characterized by X-ray diffraction (XRD), surface area (BET), transmission electron microscopy (TEM), temperature-programmed

reduction by hydrogen (H₂-TPR), X-ray photoelectron spectroscopy (XPS), temperature-programmed oxygen isotopic exchange (TPOIE) as well as the activity tests for selectively catalytic combustion of NH₃. Ordered mesoporous structure of SBA-15 was well maintained even after impregnating the various metallic components. The catalytic activity of the investigated catalysts follows a trend of Cu/ > Co/ > Mn/ > Ni/ > Fe/ > SBA-15. For the different zeolites it followed the trend of Cu/SBA-15 > Cu/SBA-16 > Cu/KIT-6. Moreover, large higher oxygen mobility is achieved over the Co/SBA-15 but produced more NO_x, and Cu/SBA-15 showed the strongest oxygen mobility among the different supports. With the results indicating that Cu/SBA-15 is the proper candidate used as a catalyst for NH₃ selective combustion towards harmless N₂.

Article ID: 40023

Title: Co₃O₄ with different morphologies for catalytic combustion of CO and CH₄ and investigation the role of their diverse oxygen species with oxygen isotopic exchange reaction

Name: Ning Liu

Affiliation: Beijing University of Chemical Technology

E-mail: wangxiaodong8530@126.com

Abstract

As a typical spinel-structure transition metal, Tricobalt tetroxide Co₃O₄ has attracted considerable attention. In this study, the Co₃O₄ samples of nanoslice(NS), nanoparticle(NP), nanoflower(NF), nanonest(NN) and nanopolyhedron(NPL) have been fabricated via the hydrothermal method and calcinating method. Physicochemical properties of the materials were characterized by means of numerous techniques (XRD, SBET, SEM, HRTEM, XPS and H₂-TPR), and their catalytic activities for CO and CH₄ combustion were evaluated. The NS and NP samples (surface area=89.6-136.7m²/g) possessed much higher surface oxygen adsorption concentrations and much better low-temperature reducibility than the other samples.

In the temperature-programmed exchange reaction, the NS sample showed the best transfer ability for surface and bulk oxygen. In the isothermal oxygen exchange reaction, the NS sample gained best transfer ability for bulk oxygen and in isothermal oxygen isotopic equilibration reaction the NS sample also showed the best transfer ability for surface oxygen. It is concluded that the excellent catalytic performance of Co₃O₄ sample was associated with its higher surface area, surface oxygen species concentration, better low-temperature reducibility and better transfer ability for surface and bulk oxygen.

Article ID: 40039

Title: Effect of hard template's residues of the nanocasted mesoporous LaFeO₃ perovskite with high surface area on methyl chloride oxidation

Name: Peixin Li

Affiliation: Beijing University of Chemical Technology

E-mail: buctywr@126.com

Abstract

Mesoporous LaFeO₃ with a superhigh surface area was prepared by mean of one-step-infiltration hard-template (HT) method, and the ordered mesoporous silica (SBA-15) was selected as HT. The final samples were characterized by XRD, TEM, XPS, XRF, Hydrogen-Temperature Programmed Reduction and Nitrogen physisorption techniques. Although TEM analysis shows the as-prepared lanthanum ferrite through the nanocasting method is not the exact replica of the corresponding HT, its surface area could reach 158 m²g⁻¹, which is much higher than that of the sample prepared by the traditional sol-gel method (< 30 m²g⁻¹). The catalytic activity was thereafter tested for catalytic combustion of methyl chloride. The influence of the HT's residues on the related combustion behaviors was investigated. By controlling the leaching time under 2 M NaOH, the different Si-residual samples were obtained. The effect of silica residues of HT on catalyst morphology & pore structure and catalytic activity has been

systematically studied. The more silica HT left in samples, the lower wide-angle diffraction peak, and the less content of absorbed oxygen species as well as the worse BET surface area and inferior activity in methyl chloride oxidation were achieved. Moreover, phenomenon of meso-structure collapsed and some new species appeared in the sample which was treated using high concentration NaOH (10M) to remove HT was observed, its BET surface area also became low.

Article ID: 40208

Title: CO₂-based polyols for sustainable polyurethane foams

Name: Thomas Müller

Affiliation: RWTH Aachen University

E-mail: thomas.mueller@tum.de

Abstract

Carbon dioxide (CO₂) is an abundant and economic resource. Using CO₂ to generate advanced polyurethane materials, which are among the most well-known polymers and widely used in foam, coating, paint and adhesive industries, is undoubtedly a sustainable way for CO₂ utilization and polyurethane industry. Polyols and isocyanates are the two main raw materials for producing polyurethanes. In the lecture, synthetic routes to CO₂-based polyols are compared and some key properties of such polyols, which enable us to produce more environmentally beneficial polyurethane materials, will be discussed.

Article ID: 40375

Title: Introduction 1,1'-butylenebis (3-methyl-3H-imidazol-1-ium) dihydrogen sulfate as an efficient Brnsted ionic liquid for the synthesis of tacrine analogues

Name: Nader Ghaffari Khaligh

Affiliation: Research House of Professor Reza. Education Guila

E-mail: ngkhaligh@gmail.com

Abstract

1,1'-butylenebis(3-methyl-3H-imidazol-1-ium) dihydrogen sulfate as an efficient, halogen-free and reusable binuclear Brønsted ionic liquid catalyzed the synthesis of tacrine analogues. This method has the advantages of high yield, clean reaction, simple methodology. The structure of the products was confirmed by IR, ¹H NMR, ¹³C NMR, Mass and elemental analysis

Oral Session II

Article ID: 40064

Title: CaIn₂O₄/Fe-TiO₂ Composite Photocatalysts with Enhanced Visible Light Performance for Hydrogen Production

Name: Jianjun Ding

Affiliation: University of Science and Technology of China

E-mail: dingjj@ustc.edu.cn

Abstract

A series of CaIn₂O₄/Fe-TiO₂ composite photocatalysts with tunable Fe-TiO₂ contents were prepared in which Fe-TiO₂ nanoparticles were uniformly deposited onto the surface of CaIn₂O₄ nanorods. The photocatalytic activities of Pt-loaded CaIn₂O₄/Fe-TiO₂ composites were evaluated for H₂ evolution from aqueous KI solution under visible light irradiation. It was found that the composites showed higher H₂ evolution rates in comparison with pure CaIn₂O₄ or Fe-TiO₂, which could be attributed to the increased surface area and enhanced visible light absorption. A high H₂ evolution rate of 280 μmol h⁻¹ g⁻¹ was achieved when the mass ratio of Fe-TiO₂ to CaIn₂O₄ was 0.5, which was 12.3 and 2.2 times higher than that of pure CaIn₂O₄ and Fe-TiO₂, respectively. Furthermore, the interfaces between CaIn₂O₄ nanorods and Fe-TiO₂ nanoparticles facilitated efficient charge separation that also led to the improved photocatalytic activity. This study may provide some inspiration for the fabrication of visible light driven photocatalysts with efficient and stable performance.

Article ID: 40074

Title: Computational Hints in Olefin Metathesis

Name: Albert Poater

Affiliation: Institut de Química Computacional i Catàlisi and D

E-mail: albert.poater@udg.edu

Abstract

In recent years olefin metathesis catalyzed by N-heterocyclic carbene ruthenium complexes has attracted remarkable attention as a versatile tool to form new C=C bonds.[1] The last developed (pre)catalysts show excellent performances, and this achievement has been possible because of continuous experimental and computational efforts to understand the laws controlling the behavior of these systems. This perspective talk rapidly traces the ideas and discoveries that computational chemistry contributed to the development of these catalysts, with particular emphasis on catalysts presenting a N-heterocyclic carbene ligand. Specifically, one of the most important challenges in ruthenium-catalyzed olefin metathesis is to increase the stability of the catalysts under reaction conditions and this hopefully without loss of activity. Special interest has been addressed to study the activation of the second-generation Grubbs catalysts, which has clarified either a dissociative or an interchange mechanism is feasible.[2] Although, in the solid state, most ruthenium-based olefin metathesis catalysts are stable to oxygen and moisture, in solution decomposition usually occurs readily. Understanding the decomposition routes of catalysts is extremely important as any insight gained in this area can guide catalyst design efforts, to participate then in the synthesis of drugs.[3,4] Furthermore, new challenging projects plan to modify the structure of the NHC ligands, or replace this ligand by alkylidene ligands, and even the substitution of the metal is a goal, moving to more environmentally friendly metals. [1] G. C. Vougioukalakis, R. H. Grubbs, *Chem. Rev.* 110, 1746 (2010). [2] C. A. Urbina-Blanco, •A. Poater, •T. Lebl, •S. Manzini, A. M. Z. Slawin, •L. Cavallo, •S. P.

Nolan, J. Am. Chem. Soc. 135, 7073 (2013). [3] S. Manzini, C. A. Urbina-Blanco, A. Poater, A. M. Z. Slawin, L. Cavallo, S. P. Nolan, Angew. Chem. Int. Ed. 51, 1042 (2012). [4] S. Manzini, A. Poater, D. J. Nelson, L. Cavallo, S. P. Nolan, Chem. Sci. 5, 180 (2014).

Article ID: 40075

Title: Ordered mesoporous carbon-titania composites as sonocatalysts: effects of frequency, power density, pH and catalyst loading dose

Name: Pengpeng Qiu

Affiliation: Korea University

E-mail: qiupengpeng22@163.com

Abstract

Herein, ordered hexagonal mesoporous carbon-titania composites were synthesized via solvent evaporation-induced co-self-assembly. The characteristics of the resulting materials were systemically investigated using small angle X-ray scattering, X-ray diffraction (XRD), thermogravimetric analysis, transmission electron microscopy (TEM), and N₂ adsorption techniques. The TEM and XRD measurements clearly showed that the composites possessed highly crystalline anatase pore walls glued by carbon to form "brick-mortar" frameworks (Fig. 1). The carbon-titania nanocomposites had a high surface area (169.94 m²/g) and a large ordered pore size (5.3 nm). The composites exhibited excellent sonocatalytic activities (much higher than those of commercial catalyst P25) for the degradation of Rhodamine B in an aqueous suspension. The effects of operating parameters such as frequency, power density, solution pH and catalyst loading dose on the sonocatalytic performance of degradation of RhB were systemically investigated

Article ID: 40098

Title: Mechanism of Photocatalytic Degradation of Volatile Organic Compounds on TiO₂: An In-situ

DRIFTS Study

Name: Fan Zhang

Affiliation: University of Science and Technology of China

E-mail: suns@ustc.edu.cn

Abstract

The adsorption and photocatalytic degradation of volatile organic compounds (VOCs), formaldehyde and toluene on TiO₂ under the different humidity levels were studied by in-situ diffuse reflectance Fourier transform infrared spectroscopy (in-situ DRIFTS) in our previous work. It was found that the formaldehyde molecules can be adsorbed on the hydroxyl groups on the TiO₂ surface via hydrogen bonding. The hydroxyl radical (OH[•]) is an effective radical which improves the mineralization rate significantly. For toluene photocatalytic degradation, the deactivation reason of TiO₂ catalysts can be attributed to the formation of stable intermediates, such as benzaldehyde and benzoic acid, which occupied the active sites on the surface of the photocatalyst. However, the adsorption structure, surface species and reaction pathways for the toluene photocatalytic degradation are still not well understood. It is worth noting that the characterization of adsorption structure of toluene weak-bonded on the TiO₂ surface is very important to determine the prior offensive position by active radicals and further elucidate the degradation mechanism therein. As known, the frequencies of bending, twisting and stretching mode of the above mentioned weak-bond are in the far infrared region. Recently, an improved in-situ far infrared DRIFTS method coupling with a homemade reaction gas-dosing system was reported and used for the investigation of gaseous toluene adsorption and photocatalytic degradation on TiO₂. It was found that toluene was adsorbed on the hydroxyl groups through the OH[•]; π -electron-type weak interaction on the surface of TiO₂ with three possible adsorption structures, ortho-, meta- and para-, instead of ipso- adsorption structure. The methyl group of the toluene is consumed first during the

process of toluene photocatalytic degradation due to the conjugation of the aromatic ring and the function of the charge transfer. An insight of the weak-bond adsorption and degradation route of toluene was proposed. Since the brightness of ordinary light source is not high enough for the investigation of weak-bond adsorption in the far-infrared region, the exact adsorption site and full explanation will be conducted with synchrotron radiation or free-electron laser to achieve higher signal-to-noise ratio.

Article ID: 40177

Title: Oxidation of Ibuprofen in sonocatalytic process by using magnetically separable TiO₂

Name: Kyounglim Kang

Affiliation: Korea Univesity

E-mail: kangkyounglim7@gmail.com

Abstract

In this research, hydrolysis and condensation reaction of Fe₃O₄, TEOS, TBT were able to synthesize the magnetically separable TiO₂ particles. Sonocatalytic degradation efficiency of IBP using the Fe₃O₄@SiO₂@TiO₂-550 and US(500 kHz) system showed that magnetically separable TiO₂ have a sonocatalytic activity.

Article ID: 40182

Title: Decolorization of Reactive Black 5 by Sonocatalytic Process with TiO₂/SWCNT Composite

Name: Jongbok Choi

Affiliation: Korea Univesity

E-mail: lic11@korea.ac.kr

Abstract

Ultrasound is eco-friendly technique, be able to apply to water treatment process. However its energy efficiency is too high to apply the large scale plant. To overcome this limitation, many researches have been performed and one of them is developing sonocatalyst. Today many papers are handled to develop novel catalyst for increasing sonocatalytic effectiveness of

ultrasound process. In early stage, researches of sonocatalysts are performed with metal oxide and pure metals. Among them, the TiO₂ is most widely used catalyst to increase degradation of pollutants in the sonocatalytic system. These days the researches of sonocatalyst are performing with composite by combining of various materials with TiO₂ using synthesis processes (sol-gel, hydrothermal etc.) In this study, to determine the optimum ratio of SWCNT(single walled carbonnanotube) with TiO₂ in TiO₂/SWCNT composite. Synthesis the catalyst was performed with hydrothermal process using hydrothermal autoclave reactor with Teflon chamber. The operating condition temperature and time of autoclave are 180 °C and 6 hrs. The Ti(SO₄)₂ solution is used for TiO₂ precursor and Single walled carbonnanotube is purchased from Sigma-Aldrich. The experiment of sonocatalytic system was used with 500 kHz and 60W. The concentration of RB5 is 10 ppm, and the concentration of RB5 is measured using UV-Vis spectrometer. The weight ratios of TiO₂ to SWCNTs used in the experiment for decolorization analysis were 1:10, 1:20, 1:100, and 1:200. Ultrasound was operated after 60min adsorption time with dark condition. SWCNT acts an adsorbent that gives surface reaction area and TiO₂ acts a photocatalyst that occurs by heat and light from cavitation phenomena. As a results, the optimum weight ratio of SWCNT and TiO₂ is 1:20.

Article ID: 40194

Title: Analysis of geometric condition for hydroxyl radical production by using stainless steel wire mesh as sonocatalyst in aqueous solution

Name: Yonghyeon Lee

Affiliation: Korea University

E-mail: hyun0415@korea.ac.kr

Abstract

Solid and inert catalyst can be the solution for fatal problems of powdered form sonocatalyst. Stainless steel wire mesh is used for solid sonocatalyst in aqueous solution. There is significant enhancement of

the production of hydroxyl radicals when absorbance of the light is compared between with-catalyst and without-catalyst. With stainless steel catalyst, absorbance is about 3 time higher than that of without catalyst.

Article ID: 40228

Title: Preparation of nano-CoOx-C supported on silican spheres with high catalytic performance for ethylbenzene oxidation

Name: zhigang liu

Affiliation: Hunan University

E-mail: liuzhigang@hnu.edu.cn

Abstract

In this study, nano-CoOx-C supported on SiO₂ (Co-TPP-SN/AC) was prepared via calcination of supported cobalt porphyrin in inert atmosphere. Characterization techniques such as FTIR, Uv-vis, SEM, TEM, XRD, N₂ adsorption-desorption and XPS etc were employed. The results showed that the catalyst consists of regular silica nanoparticles (around 300nm), and lotus-type CoOx catalysts in its surface (namely, cobalt complex in the center surrounded by the residues of carbonized metalloporphyrin) are synthesized. Moreover, the catalytic performance of Co-TPP-SN/AC for ethyl benzene oxidation were studied. Co-TPP-SN/AC exhibited an remarkable catalytic activity and selectivity (15.7% of ethyl benzene conversion and 97.8% of acetophene and phenyl alcohol). Furthermore, these catalysts could be reused 3 times without significant loss of their catalytic activity.

Article ID: 40251

Title: SiC Nanomaterials: Application to Photoelectrochemical Water Splitting

Name: Jianjun Chen

Affiliation: Zhejiang Sci-Tech University

E-mail: chen@zstu.edu.cn

Abstract

SiC nanomaterial thin film cathode for photoelectrocatalysis would have potential application in the solar production of hydrogen: the most photochemically stable semiconductors in aqueous solution, many polytypes and suitable bandgap (2.4 eV for 3C-SiC, 3.0 eV for 6H-SiC and 3.25 eV for 4H-SiC), For water splitting, water oxidation and reduction potentials lie between the valence and conduction band edges of silicon carbide. 3C-SiC nanowires were synthesized on graphite substrate by carbothermal reduction method. The high-aspect-ratio nanowires are flexible and intertwined with each other to form a porous network structure. Measurements of the diffuse reflectance of SiC semiconductor films, such as are used for water splitting, are analysed using the Kubelka-Munk radiative transfer model. Electrochemical properties of SiC nanowire film on the graphite paper substrate are investigated by cyclic voltammetry and galvanostatic charge-discharge tests, revealing ideal capacitive behavior and low contact resistance. 3C-SiC nanowire film exhibits excellent discharge capacity retention, showing excellent capacity retention. The photoelectrocatalytic water splitting to hydrogen production process is observed under visible light irradiation.

Article ID: 40293

Title: Enhanced Hydrogen Production by Ca-rich Bed-Material Coating on Olivine during Indirect Biomass Gasification

Name: Remco Lancee

Affiliation: Eindhoven University of Technology

E-mail: r.j.lancee@tue.nl

Abstract

Olivine ((Fe,Mg)₂SiO₄) is widely used as an active bed material for catalytic cracking of tars during gasification of biomass in dual fluidized bed reactors. Both the elemental composition, addition of Fe and high temperature treatments influence the catalytic properties of this mineral. Moreover, olivine is not a stable material under process conditions, relevant for

biomass gasification [1]. Formation of calcium-rich layers on olivine, due to interaction of bed material with biomass ash, has been observed during biomass gasification in dual fluidized bed gasifiers [2]. This Ca-rich layer builds-up in time, increases tar conversion and enhances hydrogen production. In our study, an olivine sample, which was coated by calcium during continuous use as bed-material in an industrial-sized indirect gasification reactor, was extensively characterized by SEM-EDS and XPS. The WGS activity was tested in a conventional fixed-bed quartz reactor, equipped with an online Mass Spectrometer. The SEM-EDS analysis of the used olivine shows significant deposition of calcium on the olivine's surface. This calcium predominantly forms on iron-rich parts of the olivine particle, suggesting that this deposition is favored by the presence of free iron-oxide. XPS combined with depth-profiling yielded detailed information on the thickness and the chemical composition of the surface layers. The Ca-rich surface layer is uniform and has a thickness of at least 0.5 μm . Moreover, an increased Fe concentration was found in the entire surface layer. The WGS activity of the Ca-coated olivine is much higher compared to fresh olivine. However, it was shown that biomass ash itself has significant WGS activity as well, which indicates that not only the bed-material coating contributes to the observed increased hydrogen-production. In conclusion, it has been shown that, when olivine is used as a reactive bed-material in industrial scale processes, a Ca-rich coating builds up on the surface of the olivine. This coating has positive effects on the overall efficiency of the process; it increases H₂ content of the product gas. This study contributes with important information on the fundamental properties of the calcium coating and its effect on the WGS reaction rate. [1] H.O.A. Fredriksson, R.J. Lancee, P.C. Thüne, H.J. Veringa, J.W. Niemantsverdriet, Appl. Catal. B: Environmental 130-131 (2013) 168. [2] F. Kirnbauer, V. Wilk, H. Kitzler, S. Kern, H. Hofbauer, Fuel 95 (2012) 553.

Article ID: 40116

Title: Study on the Basic Centers and Active Oxygen Species of Solid-base Catalysts for Oxidation of iso-Mercaptans

Name: Yufen Zhang

Affiliation: Beijing SJ Environmental Protection and New Material Co. Ltd

E-mail: zyfbuct@sina.com

Abstract

It is a challenge to remove mercaptans as well as to keep octane value in clean gasoline production. In this work, gas-liquid-solid heterogeneous base-catalyzed oxidation of tert-butyl thiol by molecular oxygen was investigated. The reactivity and stability of modified MgO catalysts were studied. The catalysts were further characterized by XRD, FT-IR, CO₂-TPD, H₂-TPD, O₂-TPD and EPR. Compared with commercial cobalt phthalocyanine catalyst (CoPc catalyst), the modified MgO catalyst displayed an enhanced stability to the oxidation of tert-butyl thiol, and the catalytic lifetime is 10 h longer than that of CoPc catalyst at 3.0 h⁻¹ of LHSV. It was found that the active sites of the catalysts are defects and basic centers. In addition, the basic sites responsible for the reactivity are mainly the medium and strong basic centers. It is interesting that part of O₃C₂--Mg₃C₂+ provide medium basic centers, however the other part of it supplies as strong basic centers. It was demonstrated that superoxide anions O₂⁻ served as the active oxygen species.

Article ID: 40081

Title: Mixed Oxides of Calcium and Zinc as Heterogeneous Catalyst in Biodiesel Production from Refined Palm Oil

Name: Carlos Alberto Guerrero Fajardo

Affiliation: National University of Colombia

E-mail: caguerrero@unal.edu.co

Abstract

Due to the additional cost and environmental problems derived from the homogeneous catalyst

re-moval in the traditional biodiesel production process, the research with heterogeneous catalysts to transesterification reaction had been increasing in the last years, and the calcium oxide had been the most promising catalyst because its high yields in the process and its low cost. The main disadvantage of this compound is its high leaching in reaction media, for this reason some researchers had found the way of supporting this oxide through the use of zinc oxide. In this work, we proposed the synthesis by co-precipitation and characterization of this catalyst in an atomic ratio Zn/Ca greater than or equal to four, also the optimization of biodiesel production operation condition, minimizing the catalyst concentration and molar ratio methanol-oil. Additionally, we analyzed the effect of the reaction over the catalyst, seeking to reuse it. In the study, it was observed that biodiesel production yields over 80% after two hours of reaction with a molar ratio methanol-oil 10:1; 5% wt catalyst and Zn/Ca atomic ratio between 4 to 4.5. This catalyst was studied by spectroscopy techniques and it was determined that it is possible to reuse it after washing with methanol and a calcination at 800 °C.

Article ID: 40171

Title: Palladium doped Perovskite-Based NO Oxidation Catalysts: The Role of Pd and B-sites for NO_x Adsorption Behavior

Name: Emrah Ozensoy

Affiliation: Bilkent University

E-mail: ozensoy@fen.bilkent.edu.tr

Abstract

Perovskite-based materials (LaMnO₃, Pd/LaMnO₃, LaCoO₃ and Pd/LaCoO₃) were synthesized, characterized (via BET, XRD, Raman Spectroscopy, XPS and TEM) and their NO_x ($x = 1,2$) adsorption characteristics were investigated (via in-situ FTIR and TPD) as a function of the nature of the B-site cation (i.e. Mn vs Co), Pd/PdO incorporation and H₂-pretreatment. NO_x adsorption on LaMnO₃ was found to be significantly higher than LaCoO₃, in line with the higher SSA of LaMnO₃. Incorporation of

PdO nanoparticles with an average diameter of c.a. 4 nm did not have a significant effect on the amount of NO₂ adsorbed on fresh LaMnO₃ and LaCoO₃. TPD experiments suggested that saturation of fresh LaMnO₃, Pd/LaMnO₃, LaCoO₃ and Pd/LaCoO₃ with NO₂ at 323 K resulted in the desorption of NO₂, NO, N₂O and N₂ (without O₂) below 700 K, while above 700 K, NO_x desorption was predominantly in the form of NO+O₂. Perovskite materials were found to be capable of activating N-O linkages typically at c.a. 550 K (even in the absence of an external reducing agent) forming N₂ and N₂O as direct NO_x decomposition products. H₂-pretreatment yielded a drastic boost in the NO oxidation and NO_x adsorption of all samples, particularly for the Co-based systems. Presence of Pd further boosted the NO_x uptake upon H₂-pretreatment. Increase in the NO_x adsorption of H₂-pretreated LaCoO₃ and Pd/LaCoO₃ surfaces could be associated with the electronic changes (i.e. reduction of B-site cation), structural changes (surface reconstruction and SSA increase), reduction of the precious metal oxide (PdO) into metallic species (Pd), and the generation of oxygen defects on the perovskite. Mn-based systems were more resilient towards B-site reduction. Pd-addition suppressed the B-site reduction and preserved the ABO₃ perovskite structure.

Article ID: 40343

Title: Niobium and Platinum-Wolframium catalysts in the conversion of furfuryl alcohol to cyclopentanone. Reaction in two steps.

Name: Ilian Guzman Velez

Affiliation: University of Basque Country

E-mail: caguerrero@unal.edu.co

Abstract

Due to the additional cost and environmental problems derived from the homogeneous catalyst re-moval in the traditional biodiesel production process, the research with heterogeneous catalysts to transesterification reaction had been increasing in the last years, and the calcium oxide had been the most promising catalyst because its high yields in the process and its low cost. The main disadvantage of

this compound is its high lixiviation in reaction media, for this reason some researcher had found the way of support this oxide through the use of zinc oxide. In this work, we proposed the synthesis by co-precipitation and characterization of this catalyst in an atomic ratio Zn/Ca greater than or equal to four, also the optimization of biodiesel production operation condition, minimizing the catalyst concentration and molar ratio methanol-oil. Additionally was analyzed

the effect of the reaction over the catalyst, seeking reuse it. In the study was observed biodiesel production yields over the 80 % after two hours of reaction with a molar ratio methanol-oil 10:1; 5 %wt catalyst and Zn/Ca atomic ratio between 4 to 4.5 . This catalyst was studied by spectroscopy techniques and was determine that is possible reuse it after wash with methanol and a calcination at 800 °C.

The 3rd Int'l Conf. on Geology and Geophysics (ICGG 2014) & The 2nd Hydrology, Ocean and Atmosphere Conference (HOAC 2014) & The 3rd International Conference on New Energy and Sustainable Development (NESD 2014)

Oral Session I

Article ID: 40028

Title: A Laboratory Study of the Effect of CO₂/Brine/Rock Interaction on Saturation Exponent of Carbonate Rocks During CO₂ Sequestration

Name: Abdulrauf Adebayo

Affiliation: King Fahd University of Petroleum & Minerals

E-mail: abdulrauf@kfupm.edu.sa

Abstract

Accurate measurements and analysis of laboratory measurements of electrical properties of core samples is a prerequisite step to the evaluation of oil and gas reserves. In recent times, this evaluation technique has been adopted in carbon dioxide sequestration projects for estimating and monitoring carbon dioxide (CO₂) accumulation in saline aquifers. Several papers have reported laboratory success in the use of resistivity measurements to monitor the flow and also estimate the volume of CO₂ plume in geological formations. Such laboratory experiments did not capture the effect of CO₂ – brine – rock interaction (CBRI) on saturation exponent and cementation factor and only

lasted for several hours or days. Determination of Archie parameters were also based on simple mathematical relations rather than on empirical relations. Two points are of immediate concern here: (i) the possibility of a change in value of saturation exponent, 'n' due to alteration in rock pore character as CO₂ sequestration last, and (ii) the procedure for determination of the Archie parameters for CO₂ estimation purpose. Preliminary results of an ongoing research work showed that a much longer experiment time accommodates CO₂ – brine – rock interaction which ultimately translated to change in pore geometry and rock resistivity as seen from NMR analysis and resistivity measurements respectively. We hereby present the results of the effect of 2 months of CO₂ sequestration in carbonate cores on saturation exponents and cementation factor. The methodology for determining Archie constants for CO₂ evaluation in CO₂ sequestration projects is also presented.

Article ID: 40062

Title: Hydro-geophysical Investigation of Contaminant Distribution at a Closed Landfill in Southwestern Ontario, Canada

Name: Jianwen Yang

Affiliation: University of Windsor

E-mail: jianweny@uwindsor.ca

Abstract

This paper presents a hydro-geophysical investigation into the landfill leachate distribution and subsurface geology at a closed site in southwestern Ontario, Canada, using geophysical mapping and hydrological modeling approaches. Conductivity mapping was first conducted over the study site using a frequency-domain EM terrain conductivity meter, revealing an anomalous high-conductivity zone of about 200m (S-N) ×80m (W-E) at the western half of the site. The DC resistivity survey was then carried out at this anomalous zone with eight S-N profiles and three W-E profiles measuring 200m in length using a Wenner- α configuration. Our resistivity survey results indicate that the landfill leachate travels mainly south-eastwards over the upper aquifer, with a minor vertical component into the upper weathered portion of the silt/sand aquitard at some locations. No contamination seems to exist in the lower sand aquifer. The geophysical results were later used to develop two conceptualized models for hydrological modeling. Our numerical results predict the leachate distribution at the study site in the future, confirming that the contaminant will occupy the entire upper aquifer and the most of the aquitard in a time of 1000 years, and that the barrier of the aquitard will protect the lower sand aquifer from the leachate pollution. These findings are critical in evaluating the current leachate conditions and the existing compliance monitoring plan for potential implementation at this study site and other sites in elsewhere.

Article ID: 40111

Title: The new Data on Stratigraphy of the Riphean Stratotype in the Southern Urals, Russia

Name: Victor Puchkov

Affiliation: Institute of Geology Ufimian Scientific Centre

E-mail: puchkv@ufaras.ru

Abstract

A recent series of U-Pb age determinations of zircons (SHRIMP, IDTIMS) from volcanic flows of several levels permitted to refine stratigraphy of the Riphean of Bashkirian megaanticlinorium (Urals, Russia), and provide a better correlation of this straton with the International and Chinese scales of the Proterozoic.

Article ID: 40133

Title: A Statistical Model for Long-Term Forecasts of Strong Sand Dust Storms

Name: Siqi Tan

Affiliation: Covance Pharmaceutical Research & Development Co.

E-mail: siqitan1985@gmail.com

Abstract

Historical evidence indicates that dust storms of considerable ferocity often wrecks havoc, posing a genuine threat to the climatic and societal equilibrium of a place. A systematic study, with emphasis on the modeling and forecasting aspects, thus, becomes imperative, so that efficient measures can be promptly undertaken to cushion the effect of such an unforeseen calamity. The present work intends to discover a suitable ARIMA model using dust storm data from northern China from March 1954 to April 2002, thereby extending the idea of empirical recurrence rate (ERR) developed by Ho (2008), to model the temporal trend of such sand dust storms. In particular we show that the ERR time series is endowed with the following characteristics: (i) it is a potent surrogate for a point process, (ii) it is capable of taking advantage of the well developed and powerful time series modeling tools and (iii) it can generate reliable forecasts, with which we can retrieve the corresponding mean number of strong sand dust storms. A simulation study is conducted prior to the actual fitting, to justify the applicability of the proposed technique.

Article ID: 40178

Title: A drilling data-aided seismic mapping method for intermediate-mafic volcanic facies and its application in hydrocarbon exploration

Name: feng yuhui

Affiliation: Jilin University

E-mail: 645350681@qq.com

Abstract

Cross-sectional and areal distribution of volcanic facies is a key for petroleum exploration. The intermediate-mafic edifice has low height-width ratio because of low viscosity of lava, which leads to difficulties in locating buried ancient volcanic centers and in characterizing its volcanic facies configuration. Based on 1300 km² regional 3D seismic data and 255 volcanic-containing wells of the 3rd member of Shahejie Formation in the Eastern Depression of Liaohe Basin, a mapping method for intermediate-mafic volcanic facies is proposed by combination of the “geology-logging-seismic” data following the order of “point-line-plane”. The “point-line-plane” order means that the whole process of geological mapping needs to proceed in turns from the point to line, then to plane under the constraint of geological models to seismic attributes. The geological models guides the geological assignment of seismic attributes, and the seismic attributes can also be validated for the geological models. The constraint and validation processes enable a final unification in “point - line - plane” scale, and to reveal the real geological conditions. The combination of “geology-logging-seismic” data means the mapping process starts from the geological understanding and geological model, and then correlate the geological and well logging data, and well logging and seismic data. After that, the geological data and seismic data are correlated via well logging data. Finally, the integration of “geology-logging-seismic” data are realized by applying mutual restriction and validation. The 2D and 3D distribution of the volcanic facies in well-lacking area are mapped based on this method. The proposed method makes full use of available well data and related information to map

intermediate-mafic volcanic facies, thus, more reliable results could be expected. This method has been successfully applied in hydrocarbon exploration in or around volcanic rocks in Liaohe Oil Company. In order to illustrate this method in detail, six drilling wells and corresponding 187.5 km² 3D seismic data are selected from the Eastern Depression of the Liaohe Basin. 1) The 1D sequence identification for volcanic facies and corresponding volcanic eruptive stages based on drilling wells. This process includes lithological correction based on geological and drilling data, identification of volcanic eruptive stages and facies. 2) The 2D configuration of volcanic facies and eruptive stages based on seismic cross sections under the constraint of well data. This process includes the inter-well correlation of volcanic eruptive stages and facies, the inter-well correlation of volcanic eruptive stages along seismic cross section, the first level seismic facies unit, which is equivalent to the volcanic edifice or volcanic edifice composite body, identification in each volcanic stages along cross section, volcanic conduit identification in the first level seismic facies unit, the second level seismic facies unit, which is equivalent to the volcanic facies or the volcanic facies combination, identification in the first level seismic facies unit, and the filling style of volcanic facies in each second level seismic facies unit. 3) The 3D characterization of volcanic facies based on well and seismic data under the constraint of 1D and 2D results. This process includes the volcanic bodies locating with coherence properties and the volcanic facies revelation with the waveform classification properties on plane. In practice of petroleum exploration, the method proposed in this study is able to construct well-correlating cross sections, gridded maps, maps for key horizons and target volcanic bodies in three dimensions.

Article ID: 40215

Title: Application of Audio-Magnetotelluric Method for Exploration the Concealed Ore-Bodies in Yuele Lead-Zinc Ore Field, Dagan County, NE Yunnan Province, China

Name: Chuandong Xue

Affiliation: Kunming University of Science and Technology

E-mail: cdxue001@aliyun.com

Abstract

The results of recent mineral exploration in the Yuele lead-zinc mining area of Daguan County, north-eastern Yunnan province, showed that there are much early Paleozoic strata under thick late Paleozoic strata in northeastern Yunnan province, where developed some hidden salt structures (SSs), often with lead-zinc polymetallic mineralization varying degrees along the tension torsional fault (belts) or fracture (joint). The ore-bodies belong to the epigenetic hydrothermal filling vein-type deposit, and the prospecting potential is great. In this area, the superficial mineralization information displayed clear, but the deep mineralization is unknown, so the exploration work is restricted. The audio-magnetotelluric (AMT) surveying is an advantage method to characterize the size, resistivity and skin depth of the polarizable mineral deposit concealed beneath thick overburden. This paper presents the surveying results using AMT method to evaluate the concealed lead-zinc mineralization in Yuele lead-zinc ore field, Daguan county, NE Yunnan province, China. After comparing the interpretation result of AMT surveying data with the geological data and the drilling data, it is found that there is some distinct difference in resistivity and polarizable between ore-bodies hosted strata, upper strata and gypsum strata. The results show that AMT method is helpful to identify lead-zinc mineralization under this geological condition.

Article ID: 40217

Title: Magnetic Method Surveying and Its Application for the Concealed Ore-bodies Prospecting of Laba Porphyry Molybdenum Ore Field in Shangri-la, Northwestern Yunnan Province, China

Name: Nguyen Ba Dai

Affiliation: Kunming University of Science and

Technology

E-mail: nguyenbadai2001@gmail.com

Abstract

Recently, a number of large molybdenum (-copper) deposits have been discovered successively in the Laba area, Shangri-La county, northwestern Yunnan province. The investigation confirmed that there is a superlarge porphyry-skarn hydrothermal vein type molybdenum-polymetallic metallogenic system with the total prediction reservoir of more than 150 mt molybdenum. The porphyry intrusions contributed to the mineralization closely, the superficial little vein molybdenum (-copper, lead, silver) orebodies are usually located in faults and fractures, and the deep porphyry type orebodies occurred in the granodiorite porphyries, the skarn type orebodies occurred in the contact zone intruded into Triassic limestone or Permian basalts. Laba ore block is a new exploration area with great prospecting potential. In order to reduce the target area and guide the further exploration work, the magnetic method measurement about 3.3 square kilometres was carried out in the ore field. This paper presents an application of analysing the horizontal and vertical derivative, using Fast Fourier Transform (FFT) filter (FFT high-pass, low-pass, cosine roll-off, susceptibility), calculated spectra frequency energy to predict the depth and intensity of the apparent remanence magnetization of source (Hilbert). The calculated results and magnetic anomalous show that, the remanence anomaly is caused by the intrusions into the Triassic limestone and Permian basalts with small anomalies, and the depth of located source is not great. We have identified a number of positions to the three drilled well, the drilled result specify interpretation with very high accuracy. The magnetic method is helpful to identify porphyry mineralization, and judge the shape and depth of the concealed ore-bearing intrusive bodies under the similar geological condition.

Article ID: 40236

Title: Research on Determination of the Main Factors

Influencing the Gas Well Post-frac Productivity Prediction for Tight Sandstone Reservoirs Based on Factors Analysis

Name: Jiang Bici

Affiliation: Jilin University

E-mail: jiangbici@163.com

Abstract

Tight sandstone reservoirs are always with the characteristics such as low porosity, low permeability, low gas saturation, almost with no natural capacity, needing fracturing for productivity, therefore fracturing capacity prediction is very necessary. But there are so many factors, and the relations between the factor and the post-frac productivity are complex. In this study, first I conclude the total factors from the gas well stable productivity formula, then using factor analysis to look for the main factors from the logging parameters and fracturing factors parameters in SULIGE area. This study could provide basic references for the gas post-frac productivity prediction in tight sandstone reservoirs.

Article ID: 40260

Title: Global Warming Impacts on Alpine Vegetation Dynamic in Qinghai-Tibet Plateau of China

Name: Yan Qing Zhang

Affiliation: Simon Fraser University

E-mail: instca@yahoo.com

Abstract

This study is to illustrate alpine vegetation dynamics in Qinghai-Tibetan Plateau of China from simulated field experimental climate change, vegetation community dynamic simulation integrated with scenarios of global temperature increase of 1 to 3°C, and simulated regional alpine vegetation distribution changes in responses to global warming. Our warming treatment increased air temperatures by 5°C on average and soil temperatures were elevated by 3°C at 5 cm depth. Aboveground biomass of grasses responded rapidly to the warmer conditions whereby biomass was 25% greater than

that of controls after only 5 wk of experimental warming. This increase was accompanied by a simultaneous decrease in forb biomass, resulting in almost no net change in community biomass after 5 wk. Under warmed conditions, peak community bio-mass was extended into October due in part to continued growth of grasses and the postponement of senescence.

The Vegetation Dynamic Simulation Model calculates a probability surface for each vegetation type, and then combines all vegetation types into a composite map, determined by the maximum likelihood that each vegetation type should distribute to each raster unit. With scenarios of global temperature increase of 1 to 3°C, the vegetation types such as Dry Kobresia Meadow and Dry Potentilla Shrub that are adapted to warm and dry conditions tend to become more dominant in the study area.

Article ID: 40271

Title: Diabase development characteristics of Eastern Depression of Liaohe Basin and its relationship with fracture

Name: Ang Sun

Affiliation: Jilin University

E-mail: 24219649@qq.com

Abstract

Observe the eastern sag of Liaohe Basin 21 core wafers of diabase, 65 wafers of debris of diabase, which found that the reservoir space of diabase are mainly dissolution pores, dissolution seam, besides by observing, Diabase depth position of well is implemented. Summarizes the characteristics of logging of diabase, it plays a positive role for failure to take samples to identify diabase of well. Based on analysis of the seismic characteristics of the well that diabase with strong amplitude, in - low frequency, phase axis continuity of good features, according to these characteristics, diabase was tracked every 5 survey lines on seismic sections starting from wells containing diabase so that established a regional diabase distribution. Diabase

mainly in Formation Shahejie Member I and Formation Shahejie Member III. Three diabase blocks were tacked in Formation Shahejie Member I, four diabase blocks were tacked in Formation Shahejie Member III. Besides through the estimates, obtain diabase intrusion distance from the fault. You can see that in this region the size of diabase intrusions in Formation Shahejie Member I to be larger than the size of diabase intrusions in Formation Shahejie Member III. From the matching relationship between diabase intrusions and fracture, the diabase intrusions in this region is mainly controlled by Jiazhangsi fracture and Jiadong fracture, distributed along this two fractures.

Article ID: 40300

Title: Ophiolite belts of the Taimyr peninsula

Name: Alina Proskurnina

Affiliation: VSEGEI

E-mail: kittine@yandex.ru

Abstract

The Taimyr foldbelt is traced along Kara Sea coast for almost 1000 km and has a key position among the main structures of the Arctic region. Observation of data permits to generalize tectonic and geochemical position of the Taimyr ophiolites

Article ID: 40340

Title: Natalka Gold Deposit

Name: Elena Nikitenko

Affiliation: NEISRI FEB RAS

E-mail: mihalitsina@neisri.ru

Abstract

Were taken studied of ore-bearing rocks, ores and gravity concentrates from Natalka gold deposit by a set of complex methods including mineralogical, petrographic and geochemical research, gravity concentration, and electronic microscopy. The major form of Au found is native: free gold is larger and dispersed, in the form of microinclusions. The obtained results are the basis for an effective

technology to extract gold and sequence of profitable mining of Natalka deposit.

Article ID: 40352

Title: Anaerobic digestion of olive oil mill wastewater pre-treated with catalytic wet peroxide photo-oxidation using copper supported pillared clay catalysts

Name: rym BEN ACHMA

Affiliation: Laboratoire de Chimie des Matériaux et Catalyse

E-mail: rymbenachma@yahoo.fr

Abstract

Because phenolic compounds are toxic for methanogenic bacteria many problems concerning the high toxicity and biodegradability of the olive oil mill wastewater (OMW) have been encountered during anaerobic treatments of this effluent. In this work, we try to develop a new catalytic process for the degradation of phenolic compounds, producing less toxic OMW for methanogenic bacteria, facilitating the anaerobic digestion. This process consists of an oxidative reaction using copper supported on alumina pillared clay in presence of a photocatalytic system (H₂O₂ with UV light). Preliminary results showed that the use of the copper supported catalyst in presence of 0.88% H₂O₂ (v/v) allows after 2 h colour reduction (25%), significant abatement of total organic carbon (40%), and important removal of polyphenolic compounds (63%) especially those of high molecular mass and subsequently decreases the OMW toxicity from 100% to 70%. This catalytic pre-treatment process of OMW was efficient for anaerobic digestion.

Article ID: 40357

Title: Planktonic foraminifera diversity in the Sea of Okhotsk and correlation to past climate change

Name: Alexandra Romanova

Affiliation: Far East Geological Institute

E-mail: sandra_ru@bk.ru

Abstract

80 sediment stations and 4 sediment cores collected in the Sea of Okhotsk were used in this study in order to reveal additional proxy for past climate reconstruction based on planktonic foraminifera. Variation in diversity indices (Simpson, Shannon and equitability indices) along the sea became additional criteria for 5 biogeographical provinces based on planktonic foraminifera. All of them show different structure aspects of the planktonic foraminifera assemblages that is very informative in cases of high relative abundance of *N. pachyderma* sin. and influence of carbonate dissolution factor. During the last 100 ky the diversity indices were changed and we can assume the migration of biogeographical provinces borders: border of the Northern province were moved to the central part in cold MIS 2,4, structure of assemblages during MIS 3, 5 was close to the modern Central province but characterized by low total foraminiferal abundance in the sediments. The Simpson and Shannon indices are more sensitive to changes in structure of planktonic foraminifera assemblages when equitability index vary lightly during the Late Pleistocene-Holocene.

Article ID: 40362

Title: Diatoms from Middle Miocene continental deposits of Primorye

Name: Olesya Likhacheva

Affiliation: Far East Geological Institute FEB RAS, Vladivostok

E-mail: olesyalikh@gmail.com

Abstract

Diatoms from Middle Miocene deposits of Khanka Lake's northwestern shore (Primorye) were studied using light and scanning microscopes. The analyses of diatom flora composition and species diversity showed that there was a dominate of several taxa that made possible the recognition of two diatom complexes. The lower complex differs from the upper one by higher species diversity, by presence of many subtropical diatoms and absence of pronounced

dominant species. Differences between the complexes can be explained by the progressing climatic cooling and predominance of fluvial-lakustrine sedimentation over the typically lake one due to development of a wide system of river valleys.

Article ID: 40257

Title: Porosity Calculation of Tight Sand Gas Reservoirs with GA-CM Hybrid Optimization Log Interpretation Method

Name: Ya-nan DUAN

Affiliation: Jilin University

E-mail: 116025147@qq.com

Abstract

Due to the additional cost and environmental problems derived from the Tight sand gas reservoirs are our country fairly rich unconventional natural gas resources, and their exploration and development is of prime importance. Sulige Gas Field which located in the northern Ordos Basin is tight sand gas reservoir, is typically featured by low porosity and low permeability, and the error of porosity calculation by traditional methods is larger. Multimineral explanation model is built by analyzing the thin slice data, and the objective function is got according to the concept of optimization log interpretation method. This paper puts the Genetic Algorithm and the Complex Algorithm together to form the GA-CM Hybrid Algorithm for searching the optimal solution of the objective function, getting the porosity of tight sandstone gas reservoirs. The deviation got by this method is lesser compared with the core porosity, with a high reliability.

Article ID: 40369

Title: Geochemistry and Petrography of Alkaline rocks from Monte Santo Alkaline Intrusive Suite, Western Araguaia Belt, Tocantins State, Brazil

Name: Rubia Ribeiro Viana

Affiliation: Federal University of Mato Grosso

E-mail: rubia@cpd.ufmt.br

Abstract

The Monte Santo Alkaline Intrusive Suite (MSAIS) is an association syenite foid, nepheline syenite and syenite. The MSAIS rocks are intruded in metapelites of the Rio do Coco meta-volcanic-sedimentary Sequence and are abundant pegmatoid veins cutting all of them. The mineral paragenesis is represented by aegirina, arfvedsonite, albite and nepheline, crystallized during the initial phase of crystallization. A late magmatic phase show nepheline, perthite, calcite and biotite, and a hydrothermal phase allowed for the formation of cancrinite, sodalite, analcime and natrolita associated with altered nepheline. The geochemical analyses showed metaluminous and medium to high potassium characteristics, being classified as miaskitic rocks, according to agpaicity and the $Na+K>1/6Si$ indexes. However, the mineralogical assemblage suggest a low to medium agpaicity composition, which can be related to a transition from miaskitic to agpaicity crystallization regime. The rare earth elements showed depletion in heavy rare earth and a strong negative Eu anomaly and enrichments in the some lithophile elements, suggesting a differentiated pattern later, which can be associated to metasomatic alterations.

Article ID: 40047

Title: Viscosity of kimberlite and basaltic magmas at the origin, ascent and eruption

Name: Eduard Persikov

Affiliation: Institute of Experimental Mineralogy RAS

E-mail: persikov@iem.ac.ru

Abstract

Diamonds carrier kimberlite magmas will ascend from mantle to the crust with the essential acceleration. Viscosity of kimberlite magmas will decrease by about 1.5 orders of magnitude during their evolution and the ascent from mantle to the crust in spite of considerable decreasing of the magmas temperature (about 300 oC), magmas partly degassing and crystallization during such processes. Kimberlite melts

can be generated in the upper mantle at the small degree of partial melting of carbonated peridotite (< 1.0 %) at pressures about 8 GPa, depths ~ (150 - 300 km), temperature ~ 1500 钛 and water content in such melts about 8.0 wt. %: ?瓮-) = 1.5 wt. %, ??? = 6.5 wt. %. Viscosity of such melts will high enough (~ 650 Pa 晧) at those parameters. But viscosity of near ?surface kimberlite melts will be much lower (~ 14 Pa 晧) at the formation of kimberlite pipes, dykes and intrusions at the pressure ~ 50 MPa, temperature ~ 1180 钛, volume contents of crystals $V_{cr.} = 0.3$ and bubbles $V_{fl.} = 0.35$, and water content in melts ?瓮-) = 1.0 wt. %. On the contrary, the viscosity of basaltic magmas will increase by more than 2.0 orders of magnitude during their evolution and the ascent from the mantle to the Earth 担 crust. Viscosity of basaltic magmas which can be generated in the asthenosphere will have minimum value (~ 1.5 Pa.s) at pressures (4 ?5) GPa, depths ~ 100 km, temperature ~ 1400 钛, and water content in such melts ?瓮-) = 0.5 wt. %. But at the final stage of evolution, for example during volcanic eruption, the viscosity of basaltic magma will considerably increase (~ 650 Pa 晧) at pressure ~ 10 MPa, temperature ~ 1180 钛, volume contents of crystals and bubbles in melts $V_{cr.} = 0.3$, $V_{fl.} = 0.15$, and water content in melts ?瓮-) = 0.5 wt. %. It has been also established that dissolution of water in basaltic and kimberlite magmas has no principal influence on the dynamics of viscosity of such magmas during the processes of origin, evolution and the ascent from mantle to the crust. These fundamental results have been established for the first time on the base of experimental and theoretical data on viscosity of magmatic melts in the series of basic - ultrabasic compositions, and using a new structural chemical model to calculate and predict the viscosity of magmatic melts [Persikov, 2007; Persikov and Bukhtiyarov, 2009].

Article ID: 40012

Title: Fractal Analysis of Dykes of the Satpura Gondwana Basin, Central India

Name: Chandan Chakraborty

Affiliation: Indian Statistical Institute

E-mail: chandan@isical.ac.in

Abstract

In the Satpura Gondwana basin of central India, dolerite dikes occur profusely with varying outcrop lengths. We have analysed the nature of their length-size and orientation distributions in relation to the theory of fractals. Two orientational sets of dikes (ENW–WSW and E–W) are present. Both the sets show strongly non-power-law size distributions, as reflected in non-linear variations in logarithmic space. We analyzed 436 number of data, revealing that polynomial functions with a degree of 3 to 4 are the best representatives of the non-linear variations. Orientation analysis shows that the degree of dispersions from the mean trend tends to decrease with increasing dike length. The length-size distributions were studied by simulating fractures in physical models. Experimental fractures also show a non-power-law distribution, which grossly conforms to those of the dolerite dikes. This type of complex size distributions results from the combined effects of nucleation, propagation and coalescence of fractures.

Article ID: 40348

Title: Some mass migration underground found in Beijing Area

Name: Jinsong Ping

Affiliation: National Astronomical Observatories, CAS

E-mail: jsping@bao.ac.cn

Abstract

The relationship between the change of a local gravity field and the mass migration underground is discussed by means of using a point-source disturbed body as a substitute for the mass migration underground. Some significant local gravity field change in Beijing area have been found, from which the three parameters of the disturbed bodies, location, depth and mass, have been derived successfully from the observations of a gravimetric network. In order to

determine the depth of a body, a new approach is suggested in which the gravity change difference is used instead of the gravity change itself. The mass of a disturbing body has been estimated properly. Astronomical PZT is suggested for this kind of survey. The results provide us a picture of the underground mass migration with which the gravity changes on the ground surface may be interpreted in a better way. This additional information may be useful in seismological studies.

Article ID: 40174

Title: A promising way of resource utilization in china: converting waste oils and fats to biodiesel

Name: Shitao Liu

Affiliation: Kunshan Innovation Institute of Nanjing University

E-mail: liust@njukii.com

Abstract

Most of Biodiesel, a clean burning alternative fuels for diesel engines is made from renewable agricultural feedstock, such as rapeseed oil, soybean oil etc., but less expensive biodiesel can also be made from waste oils and fats, including recycled restaurant grease and animal fats. Because of the eating habit of the nation and diet culture in china, restaurant-kitchen garbage is increasingly serious and has negative impact on environment and food security. The utilization of waste oils and fats to biodiesel provide a promising way of how to appropriately and effectively dispose of restaurant-kitchen garbage. This paper first review the development status of biodiesel industry, then introduce the novel technology of tubular reaction for producing biodiesel from waste oils and fats on the typical industrialization case in Kunshan. All these efforts are expected to provide a viable development path for our waste oil to produce biodiesel and worth reference to waste oils and fats recycling and reuse.

Article ID: 40359

Title: The design of stall-regulated wind turbine blade

for a maximum annual energy output and minimum cost of energy based on a specific wind statistic

Name: WIKANDA SRIDECH

Affiliation: Suranaree University of Technology

E-mail: winona13_me@hotmail.com

Abstract

The design of a stall-regulated wind turbine to achieve a maximum annual energy output is still a formidable task for engineers. The design could be carried out using an average wind speed together with a standard statistical distribution such as a Weibull with $k = 2.0$. In this study a more elaborated design will be attempted by also considering the statistical bias as a design criterion. The wind data used in this study were collected from three areas of the Lamta-kong weather station in Nakhonratchasima Province, the Khaokoh weather station in Phetchaboon and the Sirindhorn dam weather station in Ubonratchathani, Thailand. The objective is to design a best aerodynamic configurations for the blade (chord, twist and pitch) using the same airfoil as that of NREL Phase VI wind turbine. Such design is carried out at a design wind speed point. Wind turbine blades were optimized for both maximum annual energy production and minimum cost of energy using a method that take into account aerodynamic and structural considerations. The work will be carried out by the program "SuWiTStat" which was developed by the authors and based on BEM Theory (Blade Element Momentum). Another side issue is the credibility of the Weibull statistic in representing the real wind measurement. This study uses a regression analysis to determine this issue.

Article ID: 40264

Title: Optimization of Anaerobic Digestion Process to Obtain Biogas from Date Palm Tree Wastes

Name: Siddig H. Hamad

Affiliation: King Saud University, Saudi Arabia

E-mail: faljuhaimi@ksu.edu.sa

Abstract

Saudi Arabia is one of the largest producers of date fruits in the world and hence huge quantities of date palm tree waste (DPTW) are produced. We used DPTW for the production of energy in the form of biogas through an anaerobic digestion (AD) process. Appropriate ADbioreactors were designed by the team and fabricated locally. These bioreactors included a simplified model in which the contents were shaken manually whereas a more sophisticated one was equipped with a mechanical stirrer. DPTW used contained 80-90% volatile solids, which makes it quite suitable for biogas production. A starter culture was developed from thermotolerant bacteria of cow dung from King Faisal University farm. Optimum operational parameters of AD were: 40°C digestion temperature, 10% volatile solid concentration in digester slurry, 2-4 mm substrate particle size, initial pH of 7.0, 0.75% alkali pretreatment of feedstock, 30:1 C:N ratio and intermittent mixing/stirring. The best biogas yields (Liter biogas containing 50-70% methane per kg volatile solids) obtained from different parts of the tree were: Stem: 581, Leaf: 788, Fruit holder 778, Leaf stalk 867 and whole tree mixture 913. Reduction in the organic matter content of substrate after digestion was up to 58%. Reduction in the contents of cellulose, hemicellulose and soluble organic compounds after digestion was up to 68.7, 73.4 and 71.9%, respectively while lignin content was not affected. It was observed that there was minimal microbial growth during digestion which indicated that most of the organic matter consumed was converted into metabolic by products of which methane was the major component.

Article ID: 40361

Title: Enhancements of Roof Solar Chimney Performance for Building Ventilation

Name: PORNSAWAN TONGBAI

Affiliation: Suranaree University of Technology

E-mail: ptongbai@hotmail.com

Abstract

A roof solar chimney (RSC) is an inclined in the roof

of a building wherein solar radiation is employed to heat the air the channel. The hot air flows up the channel which can be used to induce flow out of the building in order to ventilate it. In this study, parameters that affect the performance of this natural ventilation system were investigated numerically, namely: inclination angles, channel gaps, solar intensities, vertical chimney attachment heights and channel expanding angles. The two last parameters were new concepts that seem to have never been studied before. All of the mentioned parameters were found to exhibit positive effects on the ventilation. Relative merits of these techniques were compared and discussed.

Oral Session II

Article ID: 40071

Title: Seismic Structure of The European Crust and Upper Mantle Based on Adjoint Tomography

Name: Hejun Zhu

Affiliation: UT Austin

E-mail: hzhu@jsg.utexas.edu

Abstract

We present a new crustal and upper mantle model for the European continent and the North Atlantic Ocean, named EU60. It is constructed based on adjoint tomography and involves 3D variations in elastic wavespeeds, anelastic attenuation, and radial/azimuthal anisotropy. Long-wavelength elastic wavespeed structure of EU60 agree with previous body- and surface-wave tomographic models. Some hitherto unidentified features, such as the Adria microplate, naturally emerge from smoothed starting model. Subducting slabs, slab detachment, ancient suture zones, continental rifts and back-arc basins are well resolved in EU60. For anelastic structure, we find an anti-correlation between shear wavespeeds and anelastic attenuation at shallow depths. At greater depths, this anti-correlation becomes relatively weak, in agreement with previous attenuation studies at global scales. Consistent with radial anisotropy in 1D

reference models, the European continent is dominated by features with radially anisotropic parameter $\xi > 1$, indicating the presence of horizontal flow within the upper mantle. In addition, subduction zones, such as the Apennines and Hellenic arcs, are characterized as vertical flow with $\xi > 1$ at depths greater than 150 km. For azimuthal anisotropy, we find that the direction of fast anisotropic axis is well correlated with complicated tectonic evolution in this region, such as extension along the North Atlantic Ridge, trench retreat in the Mediterranean and counter-clockwise rotation of the Anatolian Plate. The “point spread function” is used to assess image quality and analyze tradeoff between different model parameters.

Article ID: 40094

Title: A Generalized Optimal 17-point Scheme for Frequency-domain Scalar Wave Equation

Name: Xiangde Tang

Affiliation: Chinese Academy of Sciences

E-mail: tangxiangde@mail.iggcas.ac.cn

Abstract

Frequency-domain modeling is the basis of frequency-domain full waveform inversion. The rotated optimal 9-point scheme is an efficient algorithm for frequency-domain wave equation simulation, but this scheme fails when directional sampling intervals are different, and is only of second-order accuracy. To overcome the restriction on directional sampling intervals and low-accuracy seismic imaging of the rotated optimal 9-point, we introduce a new finite-difference algorithm, namely generalized optimal 17-point scheme. Based on an average-derivative technique, the new algorithm uses a 17-point operator to approximate spatial derivatives and mass acceleration term. The coefficients can be determined by minimizing phase-velocity dispersion errors. This generalized optimal 17-point scheme applies to equal and unequal directional sampling intervals, and can be regarded as a generalization of the rotated 17-point scheme. The number of grid

points per smallest wavelength is reduced to 2.4 by this scheme for equal and unequal directional sampling intervals. In order to suppress the reflection from the boundary, we apply a perfectly matched layer boundary condition. Numerical test on complex model further confirms the feasibility of the generalized optimal 17-point scheme.

Article ID: 40096

Title: Late Cretaceous Sub-Marine Fan System in Batain Melange Zone, Fayah Formation in South Oman

Name: Iftikhar A. Abbasi

Affiliation: Sultan Qaboos University

E-mail: iftikhar@squ.edu.om

Abstract

The Batain coast along the northeastern margin of Oman between Ra's Al-Hadd in north and Ra's Madrekah in the south is comprised of Permian to Late Cretaceous complex stratigraphy in a tectonically deformed area recording Permian rifting to late Cretaceous Tethys closure events. These rocks are thrust over Mesozoic and older autochthonous sedimentary cover of the margin in the form of a major nappe structure known as Batain Nappe. The uppermost part of the Batain nappe is comprised of isolated outcrops of early Maastrichtian siliciclastic Fayah Formation dominated with gravity flow deposits. A section near Jabal Fayah (type-section) is measured and described here for its lithofacies association to interpret the depositional system and its tectonic significance during the closure of Tethys Ocean along the northeastern margin of Oman. The Fayah Formation in Jabal Fayah area is over five hundred meters thick and is comprised of five distinct facies associations; namely, i) coarsening-up sandstone, ii) conglomerate, iii) debris-flow, iv) turbidite, and v) inter-bedded sandstone and shale lithofacies. These lithofacies are repeated many times in the section. The sandstone lithofacies association exhibits coarsening upward trend making tens of meters thick sequences in various parts of the

formation. The waterscape structures are common along with occasional sandstone dykes and convolute bedding reflecting fluidized conditions of deposition. The conglomerate lithofacies association is comprised of a series of interbedded coarsening upward pebble to gravel size conglomerates containing chert, limestone, granite and volcanic clasts ranging a few mm to cm in diameter. Occasionally these are interbedded with sandstone lithofacies. The conglomerate lithofacies was deposited by high-energy channelized flow in sub-aqueous setting. The debris-flow lithofacies association is matrix supported chaotic mixture of clay and boulders of granite, limestone and volcanic rocks, some of which are meter size in diameter, possibly derived from the nearby basement rocks such as Jabal Ja'alan basement rocks. It constitutes the most dominant part of the formation. These sediments were deposited along slope setting possibly as olistostrome formed due to submarine slumping and sliding. Turbidite lithofacies association is comprised of tens of meters thick monotonous grayish-green to brown colour clays interbedded with thin clean well-sorted sandstone. Inter-bedded sandstone and shale lithofacies association is comprised of one to half a meter thick cross-bedded, burrowed arkosic sandstone and plane laminated shale. The sandstone constitutes about 25% of the association with ripple lamination in the upper part of the unit indicating a fining-upward trend. Dewatering structures are common. This association makes up 100m of the formation. These sediments were deposited in shallow water conditions by channelized flows. Based on the above described lithofacies associations, especially the dominance of debris-flow units and turbidites, most part of the Fayah Formation are interpreted to be deposited under sub-marine fan setting. Only the upper part of the formation was deposited in shallow water setting before the onset of overlying carbonate deposits. The sub-marine fan system was active during the last stages of Tethys Ocean closure at the time of onset of Batain nappe.

Article ID: 40099

Title: Well site selection of SK-Iie, Series ICDP Project in Songliao Basin

Name: Xuejiao Qu

Affiliation: Jilin University

E-mail: quxuejiao2008@aliyun.com

Abstract

Series ICDP Project has and will practice in Songliao Basin, NE China. SK-Iie is one of the most important part of this project, and starting in 2014. The goal of the SK-Iie drilling is to obtain 3655m coring with 6400m drilling from the Huoshiling(J3) to Yingcheng Formation(K1). This project will provide unique opportunities for the geoscience community to understand the response of terrestrial environment to geological events related to the carbon cycle and greenhouse climate change, based on core already recovered and other Cretaceous terrestrial sedimentary and paleontological records there. According to the scientific objectives, drilling strategies, we are certain that our proposed drill site lies within the Xujiaweizi Fault Depression. where all target strata can be found and preserved best. There are 2 candidate areas includes Anda area and Songzhan area in the northern part of the Xujiaweizi Fault Depression, where the principles of the site selection criteria can be best met, i.e., the most complete strata and least thickness in order to reduce the engineering expenses. 3D seismic investigation has been conducted for both areas, which allows us to estimate the thickness of each formation and better meet the drilling goals; also allows us to understand the tectonic development and avoid structural complications. The strata of fault depression are characterized as complex structure, and the target layers should be dominated by fine sediments. The thickness of Yingcheng Formation and Huoshiling Formation is thin, and the Shahezi Formation with large thickness in SS3 well area, which the optimum area. Based on recently collected seismic data, lithologic information from existing cores, and discussions at the Daqing workshop, we have chosen a site for SK-Iie(125°21' 47.03" E; 46°17' 14" 26.89" N) in the north part of the basin in the Anda area of Heilongjiang

Province. The recovery ratio will be above 95%, based on SK-I core recovery. The cores will be photographed and an initial lithologic description. Thereafter, the cores will be digitally scanned, and the cores will be split (38% to be preserved as an archive). Initial sampling of the 62% of the core will take place at this time, under the supervision of a staff scientist, and open to scientists around the world.

Article ID: 40108

Title: Geological and geophysical characterization of mafic volcanic reservoirs: an example from eastern sag of Liaohe Basin

Name: Wang Yanquan

Affiliation: Jilin University

E-mail: wang_yan_quan@126.com

Abstract

Volcanic reservoirs in the eastern sag of Liaohe Basin are characterized by various types of accumulation space and complex structures, they are porous reservoirs composed of different media, including different pores, fractures and holes, and their physical properties vary greatly in space, with strong heterogeneity and changeful lithofacies. Four factors including faults, volcanic eruption cycles, lithofacies and lithology were mainly concerned about porosity and permeability in volcanic reservoirs from eastern sag of Liaohe Basin. Data base involved in the research include well-logs and corresponding geological description of 21 boreholes, analytical results of porosity and permeability of 193 rock samples, 3D seismic of the region, and structure-lithofacies mapping. 11 types of volcanic rocks were recognized and among them trachyte is the best for reservoirs development. 5 lithofacies and 14 sub-facies were classified and the extrusive facies are the most favorable ones for effective volcanic reservoirs. 5 cycles developed in the volcanic rocks, reservoir formation mainly concentrated in cycle 3, which is in the middle of volcanic cycles. The reservoir spaces can be grouped into 2 types of

primary and secondary, which can be subdivided into 9 sub-types and 14 species. Fractures of tectonic origin are the main controlling factor on permeability. Effective reservoirs are actually optimizing combination of the four factors of fracture, eruption cycles, lithofacies and lithology. Volcanic reservoirs concentrated within and around the large-scale strike-slip fault zones, especially in the conjunction of main fault and its conjugate branch. Furthermore, faults control the spatial distribution of the volcanic rocks and the development of secondary fractures. Eruption cycles control the vertical distribution of effective volcanic reservoirs. Lithofacies control reservoirs scale and primary pores development. Lithology determine the types of reservoir spaces and the intensity of alteration resulting in secondary porosity. It is significance in predicting reservoirs to clearly recognize geological and geophysical characterization for the development of volcanic reservoirs.

Article ID: 40109

Title: Element Geochemistry and Tectonic Setting of Greenschists in Central Range of Taiwan

Name: You Long

Affiliation: Jilin University

E-mail: youlong1990@gmail.com

Abstract

The Permian greenschists of the Dananao group changchun formation (so-called tailuge formation) in Taiwan are distributed in eastside of central range. Major chemical compositions of the greenschists indicate that they were originated from basalt and basaltic trachyandesite. They always contain thin interbedded marble, some of them remain pillow structure. They are characterized by high TiO₂ contents (>2%) and Ti /Y ratios (~640), the chondrite-normalized REE patterns are enriched in LREE((La/Yb)_N=3.4~9.7) with a small Eu anomaly which are similar to OIB. Their K,Rb,Sr,Ba and Cs contents vary widely (away from OIB). Based on the Zr/Y-Zr/Ti, Ti -Zr-Y and Zr-Nb-Y diagrams, the

greenschist is identified as within plate basalt (WPB). Combine with the characteristic of subaqueous eruption, the greenschists in the Taiwan province are considered to be derived from the oceanic island basalt(OIB) formed in oceanic intraplate tectonic setting. During Mesozoic period, Dananao group had undergone two different metamorphism. Tailuko belt had formed during the early metamorphism and the late metamorphism may belong to subduction along the southeast margin of Eurasian during the late Mesozoic. Our results may have important significance for further studies of Dananao group and the tectonic evolution of Taiwan.

Article ID: 40131

Title: Disastrous Flooding by the Yellow River Cannot be Prevented

Name: Michael Kimberley

Affiliation: Princeton University

E-mail: geologyone@hotmail.com

Abstract

Few people in northern Henan realize that the Yellow River is expected to produce a disastrous flood within the lifetime of the average resident. Few realize that such a flood could kill most people living in northern Henan, on the order of twenty million fatalities. Those who are not drowned in the first wave of water are expected to starve to death. It would take several weeks to bring food and water to the survivors who would be huddled in tall apartment buildings above the flood waters. By that time, everyone who has not prepared for the flood would suffer an agonizing death by starvation or a quicker death by drinking contaminated water. Despite this prediction by all known geoscientists who have examined the relevant data, virtually none of the high-rise apartment dwellers in Henan are taking the obvious precaution of storing a month's supply of water and non-perishable food. Flood waters from the Yellow River would take a few hours to reach most parts of northern Henan, so there would be enough time for nearly every apartment dweller to reach their home. Unless

attacked by starving neighbors, they would be safe there if they had enough food and water. This dire prediction is made for personal reasons. If the author is the only one in his apartment building with food and water, he must expect that thieves will break down his door. If everyone in his building has adequate provisions, he will rest peacefully until help arrives, probably a full month later. The inevitability of flooding is mostly related to variation in monsoonal rainfall but neotectonism also poses a threat, partly through the potential uplift of a small horst, like that with the carved faces of Huang and Yan, and partly through degassing of the Earth along deep-seated faults, resulting in cavern dissolution, e.g., Xuehuadong (雪花洞) at Gongyi (巩义).

Article ID: 40132

Title: Correlation among Global Climate Change, Yellow River Flooding, and Dynasty Collapse

Name: Kunhao Li

Affiliation: Princeton University

E-mail: lkhbt1@163.com

Abstract

The climate of the Northern Hemisphere has been progressively drying through the past few thousand years because the Intertropical Convergence Zone (ITCZ) has been moving southward. Increasing dryness is evident in the written history of northern Africa as well as that of China. One would think that a progressive decline in annual rainfall in the Yellow River Basin would have resulted in a progressive decline in the risk of Yellow River flooding but this has proven not to be the case. The prime reason that flooding remains a major threat to tens of millions who live in northern Henan Province is that the Yellow River has the highest sediment load of any river on Earth. Research at Delft University in The Netherlands has shown that such high sediment loads give the Yellow River tremendous erosive power. The Yellow River has more momentum per cubic meter than any other river on Earth. To use a metaphor, flooding by this river resembles a powerful train that

has jumped its tracks. Like a derailed freight train, the river may move chaotically, destroying everything in its unpredictable path. Through avulsion, the Yellow River readily may create a new course and drown all animals along that new course. We have correlated historic evidence of Yellow River flooding with historic evidence of climate change that has induced this flooding, as well as historic evidence of some political consequences of the flooding. We compare the flooding-induced collapse of Chinese dynasties to the Icelandic-eruption-induced collapse of the French Monarchy, i.e., the French Revolution that heralded the Napoleonic Era.

Article ID: 40333

Title: New data on trace element geochemistry of the Gaussberg leucitites (West Antarctica)

Name: Natalya Migdisova

Affiliation: Vernadsky Institute for Geochemistry

E-mail: nat-mig@yandex.ru

Abstract

Olivine leucitites of late Cenozoic age form the Gaussberg extinct volcanic cone on the coast of the Antarctic ice sheet within Gaussberg rift zone possibly being a part of Lambert fracture zone. Samples gathered during 2nd Soviet Antarctic Expedition (1957-1958) are mostly pillow lavas with a well defined black glassy crust. New high precision data on selected lamproitic samples from Gaussberg volcano (Antarctica) including rare elements in olivine phenocrysts, clinopyroxene phenocrysts coupled with whole rock and quenched glass rare and main elements patterns show distinct features of continental ultra-potassium alkaline magmatism. Isotope systems (Pb, Sr, Nd) indicate a LOMU type primary mantle. According to isotopic data Gaussberg melting source is ancient Gondwana lithosphere (in East Antarctica). Crystal fractionation is one of the major processes affecting the composition of magmas. Investigations in lamproitic magmatism are important for understanding the geochemically anomalous reservoirs in mantle. Gaussberg leucitites are the rocks

with unusual petrologic composition ($K_2O \gg Al_2O_3$; high SiO_2 content at given MgO) implying non-uniform melting source [1, 2]. Mineral assemblage is 60% Lct, 30% Ol, 10% Cpx. Trace element patterns of Gaussberg quenched glass samples have extreme enriched character. Maxima on Ba, La, Pb and Zr-Hf maxima are typical features of continental lithosphere [1]. In this study we report the Gaussberg mineral collection [3]. Two types of Cpx phenocrysts were detected in Gaussberg: (1) high TiO_2 , low Al_2O_3 group and (2) low TiO_2 , high Al_2O_3 group. Detailed electron probe microanalysis (ISTerre Universit ; J. Fourier-CNRS, Grenoble, France) revealed the inverted zone character of Cpx grains – the core is enriched in FeO and depleted in Al_2O_3 while the rim is enriched in Al_2O_3 and depleted in FeO. Obviously Cpx imprinted the mix of two different melts. These melts can indicate the two stages of crystallization in Gaussberg magmatic system. Leucite is the most abundant phenocryst in Gaussberg lavas. Leucite fractionation is restricted in near surface magma chambers. Gauss leucites are enriched in Na_2O (0,1-0,28 wt%) and depleted in K_2O (20,7-20,2 wt%) and FeO (0,7-1,2 wt%) compared to the leucites from another lamproite provinces. Gaussberg olivine is high magnesium (up to Fo93). Coefficients of olivine/liquid distribution were calculated based on new high precision data on minor elements (Li, Al, Ca, Cu, Zn, Si, Sc, Ti, V, Cr, Mn, Co, Ni, Ga, Ge, Sr, Y, Zr, Mo, Ce, Nd, Gd, Dy, Er, Yb) in olivine and corresponding quenched glasses (GEOMAR Helmholtz Centre for Ocean Research, Kiel, Germany). Determined coefficients $K_{Dol/Liq}$ are the larger for Ni (73) > Co (5) > Mn (1,2) > Zn (0,8) > Li (0,5) > Cu (0,02) and other non compatible lithophile elements. Gaussberg olivine has high Ni/Co ratios (20-40) implying the melting under the thickened lithosphere [4]. These results make a contribution to lamproite’s database expanding the data for weakly studied (due to their rarity) leucitite rocks. Gaussberg volcano mantle source is enriched in $^{207}Pb/^{204}Pb$ and $^{208}Pb/^{204}Pb$ while it has low $^{206}Pb/^{204}Pb$ (≈ 17.5) value. High $^{87}Sr/^{86}Sr$ ($\approx 0.707-0710$) taken together with low $^{143}Nd/^{144}Nd$

(≈ 0.5119) ratios suggest LOMU-type of primary mantle source. Isotopic data reveal that Gaussberg volcano melts source was the ancient Gondwana lithosphere but not the Antarctic mantle source (Mesozoic plumes).

Article ID: 40334

Title: Interpretational Applications of Spectral Decomposition in Diabase Fractures Prediction

Name: Qiao Wang

Affiliation: Jilin University

E-mail: 369594859@qq.com

Abstract

As the dominant frequency of the seismic data in the eastern sag of the Liaohe oilfield igneous is very low (13-20Hz), this brings a problem in igneous fractures prediction. To solve this problem, this paper uses spectral decomposition and gets success. Minor fractures of full-bandwidth seismic data is usually not obvious, we propose to predict the minor fractures using dominant frequency seismic data by spectral decomposition. Meanwhile, in order to avoid the effect caused by lithological differences, in this paper, we choose a single lithology, diabase, to predict fractures. The result of fractures prediction is accord with the well’s fluid-filled property, and spectral decomposition is more accurate than coherent. Compared with other methods, this technology can be used in the low dominant frequency seismic data, and it is more clearly in fractures prediction, is easier to conduct, save more time, have no logging-constrained. This technology can provide important reference in late reservoir evaluation and well deployment.

Article ID: 40317

Title: Flood Risk for Embanked Rivers

Name: Ewa Bogdanowicz

Affiliation: Institute of Meteorology and Water Management

E-mail: Ewa.Bogdanowicz@imgw.pl

Abstract

Flood frequency analysis (FFA) concentrates on peak flows of flood hydrographs. However, floods that last years devastated large parts of Poland lead us to revision of the views on the assessment of flood risk in Poland. It turned out that it is the prolonged exposure to high water on levees that causes floods, not only the water overflowing the levee crest. This is because, the levees are weakened by water and their disruption occurs when it seems that the danger is over, i.e. after passing culmination. Two main causes of inundation of embanked rivers, namely over-crest flow and wash out of the levees, are combined to assess the total risk of inundation. Therefore the risk of inundation is the total of risk of exceeding embankment crest by flood peak and risk of washout of levees. Hence, while modelling the flood events in addition to the maximum flow one should consider also the duration of high water in a river channel, Analysis of the frequency of annual peak flows based on annual maxima and peaks over threshold is the subject of countless publications. Therefore we will here mainly modeling the duration of high water levels. In the paper the two-component model of flood hydrograph shape i.e. 'duration of flooding-discharge-probability of non-exceedance' (DqF), with the methodology of its parameters estimation for stationary case was developed as a completion to the classical FFA with possible extension to nonstationary flood regime. The model combined with the technical evaluation of probability of levees breach due to the d-days duration of flow above alarm stage gives the annual probability of inundation caused by the embankment breaking. The results of theoretical research were supplemented by a practical example of the model application to the series for daily flow in the Vistula River in Szczecin. Regardless promising results, this method is still in its infancy despite its great cognitive potential and practical importance. Therefore, we would like to point to the usefulness and necessity of the DqF models to the one-dimensional analysis of the peak flood hydrographs and to flood risk analysis. This approach constitutes a new direction in FFA for

embanked rivers.

Article ID: 40318

Title: On Return Period of the Largest Historical Flood

Name: Witold G. Strupczewski

Affiliation: Institute of Geophysics Polish Academy of Sciences

E-mail: wgs@igf.edu.pl

Abstract

The use of nonsystematic flood data for statistical purposes depends on reliability of assessment both flood magnitudes and their return period. The earliest known extreme flood year is usually the beginning of the historical record. Even though the magnitudes of historic floods are properly assessed, a problem of their return periods remains unsolved. Only largest flood (XM) is known during whole historical period and its occurrence carves the mark of the beginning of the historical period and defines its length (L). So, it is a common practice of using the earliest known flood year as the beginning of the record. It means that the L value selected is an empirical estimate of the lower bound on the effective historical length M. The estimation of the return period of XM based on its occurrence, i.e. $M \approx L$, gives the severe upward bias. Problem is to estimate the time period (M) representative of the largest observed flood XM. From the discrete uniform distribution with support of the probability of the L position of XM one gets $M \approx 2L$ which has been taken as the return period of XM and as the effective historical record length. As in the systematic period (N) all its elements are smaller than XM, one can get $M \approx 2(L + N)$. The efficiency of using the largest historical flood (XM) for large quantile estimation (i.e. one with return period $T = 100$ years) has been assessed using maximum likelihood (ML) method with various length of systematic record (N) and various estimates of historical period length M^{\wedge} comparing accuracy with the case when only

systematic records alone (N) are used. The i-th simulation procedure incorporates systematic record and one largest historic flood (XMi) in the period M which appeared in the Li year backward from the end of historical period. The simulation result for selected distributions, values of their parameters, different N and M values are presented in terms of bias (B) and root mean square error (RMSE) of the quantile of interest and widely discussed

Article ID: 40324

Title: A Study of Sediments and Radioactive Particles of the Yenisei River Using a Variety of Analytical Methods

Name: Alexander Bolsunovsky

Affiliation: Institute of Biophysics SB Russian Academy of Sci

E-mail: radecol@ibp.ru

Abstract

The Yenisei River, one of the largest rivers in the world, is contaminated with artificial radionuclides released by a Russian nuclear facility producing weapon-grade plutonium, which has been in operation for many years. Examination of Yenisei River sediment samples revealed the presence of artificial radionuclides typical of radioactive discharge from the Mining-and-Chemical-Combine (MCC) nuclear facility: isotopes of europium (^{152}Eu , ^{154}Eu , and ^{155}Eu), cesium (^{137}Cs and ^{134}Cs), ^{60}Co , ^{90}Sr , and transuranium elements. The MCC is also a source of radioactive particles in the Yenisei. New data on radionuclide concentrations in sediments and radioactive particles in the Yenisei River were obtained using a wide range of analytical methods. Sequential extraction performed on samples of sediment cores showed different degrees of potential environmental availability of artificial radionuclides and uranium. In a few samples, ^{241}Am was present in the unextractable form, which may be accounted for by the presence of microparticles of the reactor fuel. These microparticles were investigated using scanning electron microscopy, and their reactor origin was

confirmed.

Article ID: 40055

Title: Depositional and tectonic constraints for hydrocarbon targets of the Lutetian–Langhian sequences from the Gulf of Gabes — Tunisia

Name: Fatma TAKATK

Affiliation: King Saud University

E-mail: fatimtak@yahoo.fr

Abstract

The sequence stratigraphy of the Lutetian–Langhian series in the Gulf of Gabes basin was defined using cuttings from 50 wells, wireline logs, biostratigraphic data and seismic data. The seismic profiles display a shallow inner shelf passing northeastward to an outer shelf break. Our study helps constrain the depositional and tectonic constraints for hydrocarbon targets. Indeed, syndepositional tectonics and related subsidence and eustatism as well, were found to exert remarkable control on the source-rock and oil-reservoir formations and spatiotemporal repartitions. Detrital facies in the inner shelf pass seaward into a broad carbonate shelf and then into storm-influenced turbidites; whereas marls in the deep shelf and outer basin extend onto the inner-shelf during major highstands. Three major supersequences were identified and each of these comprised multiple third order sequences. The lower supersequence (Lutetian–Priabonian) contains marls interceded with inner-shelf skeletal carbonates which reflect shelf flooding due to rise in sea level. The second supersequence (Rupelian–Burdigalian) bears clays and sands admixed with foraminifered carbonates at the base. Rapid flooding and progradation of shelf carbonate sediments (Vascus Horizon and Ketatna Fm) reflect eustatic lowering. These deposits grew basinward into pelagic marls enriched in organic matter and interceded with limestones (Salammbô Fm). A variety of seismic patterns of the Ypresian–Langhian sequences, notably the concave/lens-shaped ones are associated with transparent seismic facies and are thought to be

accounted for by tectonically subsiding depositional settings. Faulting and associated subsidence have caused overlapping seismic reflection patterns of sequences dating the Lutetian to Middle Langhian times. The tectonic pulses and flower faults striking to the NW, with antithetic branches continuously reactivating in the study time interval, caused subsidence and basin margin steepening toward the northeast. In contrast, the west and southwest parts of the basin, tectonically expelled in the form of a broad paleohigh, were the sites for platform carbonates interfingering with episodes of pelagic sedimentation. A major gap of the Upper Eocene is due to a compressive tectonic period. The Ketatna Fm shows concordant and rather transparent seismic facies, thus contrasting with coeval pelagic intervals with dipping of internal seismic reflections due to intervening normal faulting. A broad transgression during the Middle Langhian deposited the third supersequence due to global warming and subsequent rise in sea level. The carbonate sequences in the Reineche Member, the Ketatna and the Aïn Ghrab formations are notably thick and are proven gas and oil reservoirs.

Article ID: 40091

Title: Low-frequency modulation and trend of the relationship between ENSO and precipitation along the Northern to Center Peruvian Pacific coast.

Name: Pedro Rau

Affiliation: GET, Universittade Toulouse III – CNRS – IRD – OMP

E-mail: pedro.rau@get.obs-mip.fr

Abstract

The relationship between ENSO (El Nino Southern Oscillation) and precipitation along the Peruvian Pacific coast is investigated over 1964-2011 based on a variety of indices accounting for the different types of El Nino events and atmospheric and oceanographic manifestations of the interannual variability in the tropical Pacific. We show the existence of fluctuations in the ENSO/precipitation relationship at decadal

timescale that are associated with the ENSO property changes over the recent decades. Several indices are considered in order to discriminate the influence of the two types of El Nino, namely the Eastern Pacific El Nino and the Central Pacific El Nino, as well as the influence of large scale atmospheric variability associated to the Madden and Julian Oscillation (MJO), and of regional oceanic conditions. Three main periods are identified which correspond to the interleave periods between the main climatic transitions over 1964-2011, that is the shifts of the 70s and the 2000s, over which ENSO experiences significant changes in its characteristics. We show that the relationship between ENSO and precipitation along the western coast of Peru has experienced significant decadal change. Whereas El Nino events before 2000 lead to increased precipitation, in the 2000s, ENSO is associated to drier condition. This is due to the change in the main ENSO pattern after 2000 that is associated to cooler oceanic conditions off Peru during warm events (i.e. Central Pacific El Nino). Our analysis also indicate that the two extreme El Nino events of 1982/83 and 1997/98 may have overshadowed actual trends in the relationship between interannual variability in the tropical Pacific and precipitation along the coast of Peru. Overall our study stresses on the complexity of the precipitation on the western side of the Andes with regards to its relationship with the interannual to decadal variability in the tropical Pacific.

Article ID: 40114

Title: The influence of water area on local climate by using COSMO NWP model

Name: Kristyna Bartunkova

Affiliation: Institute of Atmospheric Physics, ASCR

E-mail: kbar@ufa.cas.cz

Abstract

We used the COSMO NWP model to estimate the influence of newly originated water areas (lakes) on local air temperature and air humidity. The impact of the lake was simulated for a flat terrain, various

meteorological conditions and different lake sizes. The COSMO NWP model was applied with a very high horizontal resolution of 333 m and its outputs we used as “true” data for developing a simple physical-statistical model ALAKE. The ALAKE is a model for estimating impact of a future lake on its surroundings, which is easy to apply because it uses easily accessible input data. They are: a lake size, air temperature and humidity in 2m above the surface, the temperature of the mixing layer of the lake, wind speed and direction in 10 m above the surface at the given place. The ALAKE model application is very fast and therefore it allows calculating the lake impacts for various meteorological situations (e.g. for several years of data). By statistical processing of obtained results general picture of the lake impact can be obtained. The ALAKE model is planned to be used for the evaluation of the impact of hydric restoration of former open coal mines in Podkrusnohorské Valley in the Czech Republic.

Article ID: 40148

Title: The METRo-CZ model for nowcasting of road surface temperature

Name: Zbynek Sokol

Affiliation: Institute of Atmospheric Physics ASCR

E-mail: sokol@ufa.cas.cz

Abstract

The METRo-CZ model has been developed from the Model of the Environment and Temperature of Roads (METRo), which was originally developed at Environment Canada. We adapted the METRo-CZ to the conditions of the Czech Republic. In our version, the model uses online measurements from road weather stations in the Czech Republic and weather forecasts from ALADIN, the operational numerical weather prediction model of the Czech Hydrometeorological Institute. In our contribution we will present evaluation of the METRo model application in semi-operational mode. Beside that we will present a new version of the METRo-CZ model that utilizes data from the Meteosat Second

Generation for nowcasting of radiation fluxes. The impact of the satellite data will be evaluated.

Article ID: 40172

Title: The Influence of El Nino on MJO over the Equatorial Pacific

Name: Xiong Chen

Affiliation: PLA University of Science and Technology

E-mail: chenxiong198811@163.com

Abstract

In this paper, the influence of El Nino event on the MJO (Madden-Julian Oscillation) over the equatorial Pacific is studied by using reanalysis data and relevant numerical simulation results in GCM. It is clear shown that El Nino can reduce the intensity of MJO. The kinetic energy of the MJO over the equatorial Pacific is stronger before the occurrence of the El Nino event, but it is reduced rapidly associated with the El Nino outbreak and the weaker MJO even can continue to next summer. The convection over the central-western Pacific is also weaker during the El Nino, and the OLR anomaly is positive in the El Nino winter, which even has opposite temporal variation comparing to the non-El Niño case over the central-western Pacific. As El Nino event also affects the vertical structure of the MJO, so the opposite direction feature of the geopotential height and the zonal wind in upper and low level troposphere for the MJO are not remarkable in El Nino case, which is inclined to be barotropic feature. El Nino event have the influence on the eastward propagation of the MJO too. During the El Nino winter, the eastward propagation of the MJO is not so regular and unanimous and there exists some eastward propagation is faster than one in non-ENSO case. The dynamic analyses suggest that positive SSTA (El Nino case) affect atmospheric thickness over the equatorial Pacific and then the excited atmospheric wave-CISK mode is weaker, so that the intensity of MJO is reduced; and the combining of the barotropic unstable mode in the atmosphere excited by external forcing

(SSTA) and original MJO may be an important reason to lead the MJO vertical structure to inclining to be barotropic during El Nino.

Article ID: 40197

Title: Aggregation methods in flood frequency analysis

Name: Iwona KuptelMarkiewicz

Affiliation: Institute of Geophysics Polish Academy of Sciences

E-mail: iwonamar@igf.edu.pl

Abstract

Flood frequency analysis (FFA) provides information about the size of the probable flood flows. Obtained in this way, the estimates of the maximum flow quantiles have many practical applications. Among others, they are required for dimensioning hydraulic structures and for determining the limits of flood zones with varying degree of flood risk. Due to high costs of hydrological structures, the improvement of the accuracy of high flow quantile assessment is considered as the basic goal for the flood frequency analysis. In the classical approach, the problem of the flood frequency modeling refers to the choice from a set of candidate distributions such a probability distribution which the best describes the analyzed series of annual or seasonal maximum flows. However, the choice of the best fitting model (distribution type and its parameter values) is not unique. It depends on the discrimination procedure used (criterion for the selection of the distribution) and the method of estimation. Moreover, even if we decide on a subjective or imposed some guidelines choice of distribution, its type can change with the length of the measurement series. This may cause significant shifts in the upper quantile estimates, even every year, posing a huge problem for engineers and designers of hydraulic structures. To reduce the uncertainty and instability of the upper quantile estimates, the method proposed by Bogdanowicz (2010) can be applied to determine the maximum flow quantiles. In contrast to the commonly used methods of choosing the best model selection from a set of

candidate distributions, all the information contained in these distributions is aggregated here in the form of a weighted average. The original weights are evaluated on the basis of the Akaike information criterion (AIC), which bases on the maximum likelihood function of the distribution, so in fact, on the main probability mass. We propose two alternative methods sensitive in the range of the upper quantiles for defining the weights of the candidate distributions. A key element of the aggregation method is the choice of the candidate probability distributions for describing the data series of maximum flows. We analyze the impact of the number and type of the candidate distributions on the value of flood quantile estimates for the Polish data. As the complement to the commonly used flood-like distributions, the inverse Gaussian and generalized exponential density functions are investigated here. Both these models have been found to match the number of Polish data successfully. Literature: Bogdanowicz E., 2010: *Podejście wielomodelowe w zagadnieniach estymacji kwantyli rozkładu wartości maksymalnych (Multimodel approach to estimation of extreme value distribution quantiles)*, Polska Akademia Nauk, Komitet Inżynierii i Rodowiska, Monografia nr 68: *Hydrologia w inżynierii i gospodarce wodnej (tom 1)*, Komitet Inżynierii i Rodowiska PAN, 57-70.

Article ID: 40294

Title: On the Application of Probabilistic Hydrometeorological Simulation of Soil Moisture Across Different Stations in India

Name: Sarit Kumar Das

Affiliation: Indian Institute of Technology, Kharagpur

E-mail: saritkdas@iitkgp.ac.in

Abstract

An application of a proposed hydrometeorological approach for probabilistic simulation of soil moisture

is carried out. The time series of in-situ soil moisture and meteorological variables at monthly scale from a few monitoring stations having different soil-hydrologic properties across India are utilized. Preliminary investigation with both precipitation and near-surface air-temperature as meteorological variables to establish that the strength of association between soil moisture and precipitation is more significant as compared to that between soil moisture and temperature. Precipitation-based probabilistic estimation of soil moisture using the proposed hydrometeorological approach is tested with in-situ observed soil moisture, CPC model output and with soil moisture data of the Climate Change Initiative (CCI) project. The parameter of the developed model is linked to the soil-hydrologic characteristics through Hydrologic Soil Group (HSG) classification. Higher values of model parameter (dependence parameter (θ) for the selected copula) correspond to HSG A and B having higher soil porosity, whereas, lower values correspond to HSG B and C having lower soil porosity.

Article ID: 40364

Title: Tsunami Simulation of the April 01, 2014 Chile Earthquake due to Preliminary Results of Point Source and Finite-Fault Source Models

Name: Ergin Ulutas

Affiliation: Kocaeli University, Department of Geophysics

E-mail: ergin.ulutas@gmail.com

Abstract

We have simulated the tsunami generated from the 01 April 2014, Mw:8.2 earthquake. The assumed tsunami source is located due to the finite-fault source model of United States Geological Survey. The post event tsunami calculations were performed in order to better represent the event and identify more in detail the affected locations. Non-linear shallow water equations are solved with a finite difference scheme, using a computational grid over GEBCO 30 bathymetry data. The purpose of the study is to examine the differences

between preliminary parameters of point source and finite fault models on tsunami simulation. The simulated waves were also compared with the available deep ocean pressure sensors and tide gauges records along Chilean coasts. De-tiding, de-trending, low-pass and high-pass filters were applied to detect tsunami waves in deep ocean sensors and tide gauge records. Although the sea level readings immediately after the earthquake showed the earthquake generated a tsunami in near field, the observed records and results of simulations showed that the earthquake did not generate larger tsunamis than expected from its moment magnitude in the far field. The consequences of the assumptions of source characteristics on tsunami simulations may contribute to examine why the tsunami only affected local areas.

Article ID: 40368

Title: SHRIMP U-Pb and U-Pb laser ablation geochronological on zircons from Monte Santo Alkaline Intrusive Suite, Western Araguaia Belt, Tocantins State, Brazil

Name: Rubia Ribeiro Viana

Affiliation: Federal University of Mato Grosso

E-mail: rubia@cpd.ufmt.br

Abstract

The Monte Santo Alkaline Intrusive Suite (MSAIS) is an association syenite foid, nepheline syenite and syenite, which are intruded in metapelites of the Rio do Coco meta-volcanic-sedimentary Sequence, presenting abundant pegmatoid veins cutting all of them. The ages obtained by Shrimp (1051 ± 22 Ma, 1048 ± 11 Ma) are very close those younger age obtained by U-Pb laser ablation (1056 ± 21), being interpreted as crystallization age. These dating reveal also that MSAIS rocks were affected by common succession of younger events below 550 Ma ago, responsible by the later rocky bodies of varying composition occurring in the region, including the alkaline pegmatites hosted in the nepheline syenite of the MSAIS.

The 2nd Genetics and Genomics Conference (GC 2014) & the 2nd Int'l Conf. on Biomedical Engineering (ICBE 2014)

Oral Session

Article ID: 40101

Title: Genetic diversity of the PSMA6, PSMC6 and PSMA3 proteasomal genes in Latvian, Lithuanian and Taiwanese populations

Name: Tatjana Sjakste

Affiliation: University of Latvia

E-mail: tanja@email.lubi.edu.lv

Abstract

PSMA6 (rs2277460, rs1048990), PSMC6 (rs2295826, rs2295827) and PSMA3 (rs2348071) genetic diversity was investigated in 1438 unrelated subjects from Latvia, Lithuania and Taiwan. In general, polymorphism of each individual locus showed tendencies similar to determined previously in HapMap populations. Main differences concerns Taiwanese and include presence of rs2277460 rare allele A not found before in Asians and absence of rs2295827 rare alleles homozygotes TT observed in all other human populations. Observed patterns of SNPs and haplotype diversity were compatible with expectation of neutral model of evolution. Linkage disequilibrium between the rs2295826 and rs2295827 was detected to be complete in Latvians and Lithuanians ($D \text{ \& \#189; } = 1; r^2 = 1$) and slightly disrupted in Taiwanese ($D \text{ \& \#189; } = 0.978; r^2 = 0.901$). Population differentiation (FST) was estimated from loci variability, five locus haplotypes and PSMA6 and PSMC6 two locus haplotypes. Latvian and Lithuanian populations were significantly differentiated by each the rs1048990, rs2295826 and rs2295827 (PSMC6) locus. Latvians were differentiated from all Asians by each of 5 SNPs. However, Lithuanians and Asians were differentiated only by rs2277460, rs1048990 and rs2348071 and were not differentiated by PSMC6 loci.

Considering five locus haplotypes all European populations were significantly differentiated from Asian; Lithuanian population was differentiated from both Latvian and CEU. Allele specific patterns of transcription factor binding sites and splicing signals were predicted in silico and addressed to eventual functionality of nucleotide substitutions and their potential to be involved in human genome evolution and geographical adaptation. Current study represents a novel step toward a systematic analysis of the proteasomal genes genetic diversity in human populations. Acknowledgements Costs of this work were partly covered by the following projects: Latvia-Lithuania-Taiwan Cooperation No V320100512; Latvian National Research Programme 2010.10.-4/VPP4; ESF project No 2013/0043/1DP/1.1.1.2.0/13/APIA/VIAA/002.

Lithuanian team acknowledge Ministry of Education and Science and Research Council of Republic of Lithuania for financial agreements TAP 10043, TAP-06/2011 and TAP LLT 08/2012.

Article ID: 40112

Title: In Vitro Studies Of 1,4-Dihydropyridine Peroxynitrite Scavenging and Dna Protective Activities

Name: Nikolajs Sjakste

Affiliation: Latvian Institute of Organic Synthesis

E-mail: Nikolajs.Sjakste@lu.lv

Abstract

IN VITRO STUDIES OF 1,4-DIHYDROPYRIDINE PEROXYNITRITE SCAVENGING AND DNA PROTECTIVE ACTIVITIES Evita Rostoka¹, Elina Buraka¹, Larisa Baumane¹, Jean-Luc Boucher², Vitalijs Borisovs³, Nikolajs Sjakste ^{1,3} ¹Latvian Institute of Organic Synthesis, Aizkraukles 21, Riga

LV1006, Latvia 2Laboratoire de Chimie et Biochimie Pharmacologiques et Toxicologiques, UMR 8601 CNRS, Université René Descartes, Rue des Saints Pères 45, 75270 Paris, Cedex 06, France 3University of Latvia, Raiņa bulv. 19, Riga LV-1586. Latvia

Abnormal production of reactive oxygen species (ROS), DNA damage produced by free radicals and insufficient DNA repair of these damages are important in pathogenesis of several cardiovascular and metabolic diseases. Search for compounds able to scavenge toxic derivatives of free radicals and to protect DNA against damage is a topical problem. Aim of our study was to evaluate ability of some 1,4-dihydropyridines synthesized in the Latvian Institute of Organic Synthesis to scavenge peroxyxynitrite, free radicals and to protect DNA against action of ROS and their toxic metabolites. Uncoupling of NO synthases leads to overproduction of superoxide radical, it leads to development of diabetes mellitus complications and causes cardiotoxic effects of doxorubicin. Uncoupling was monitored by means of assessment of NADPH consumption by biotechnological preparations of the enzymes. 50 mM of doxorubicine increased NADPH consumption by nNOS in presence of L-Arg five-fold, without substrate - 2.2 times. Consumption of NADPH by iNOS was increased 3.6 times. 1,4-DHP (etaftorone and fenofitorone) per se did not affect the NADPH consumption. Etaftorone did not decrease increase of NADPH consumption. However fenofitorone was quite effective, it significantly reduced the increase in NADPH oxidase activity of iNOS induced by doxorubicine (IC₅₀ ~200 μM). Ability of 1,4 DHP to scavenge hydroxyl radical produced in Fenton's reaction was studied by means of ESR spectroscopy with DMPO spin label, twenty 1,4-DHP derivatives were studied. It was shown that metkarbaton was the only effective hydroxyl radical scavenger among these compounds. Some compounds (fenofitorone, AV-153-Li) were able to decrease formation of relaxed plasmid form triggered by free radicals as revealed by gel electrophoresis. Ability of the compounds to scavenge peroxyxynitrite were

monitored by measuring the rate of peroxyxynitrite decomposition, in the presence or in the absence of the 1,4-DHP, the reaction was followed was followed at 302 nm where the peroxyxynitrite anionic form absorbs, The most interesting results were obtained with lipophylic 1,4-DHPs compounds: fenofitorone, etaftorone and cerebrokrast. Cerebrokrast intensified rate of decomposition of peroxyxynitrite 8 times, fenofitorone and etaftorone- about twice. Ability of the compounds to protect DNA against peroxyxynitrite-induced damage was evaluated by gel electrophoresis of plasmids treated with peroxyxynitrite and tested compounds. Several derivatives of 1,4 – DHP: AV-153-Na, AV-154-Na, AV-153-Li decreased degree of peroxyxynitrite-induced damages in low concentrations. In comet assay etaftorone and AV-153 manifested ability to decrease level of alkali-labile sites in HeLa cells induced by peroxyxynitrite treatment. The work was supported from the European Social Foundation project "Establishment of a new interdisciplinary group to an effective treatment for diabetic nephropathy finding ways", Grant of the Latvian Council of Science 278/2012 and National Research Program 2010.10.-4/VPP4.

Article ID: 40033

Title: A novel genetic method for generation of antioxidant mice with graded gene expression

Name: Xianwen Yi

Affiliation: Xinxiang Medical University

E-mail: xyi2000@hotmail.com

Abstract

A novel genetic method for generation of antioxidant mice with graded gene expression Xu Guangcui*, Zhao Yingzheng*, Wu Weidong and Yi Xianwen School of Public Health, Xinxiang Medical University, Xinxiang, China, 453003 Oxidative stress is implicated in pathogenesis of many diseases and antioxidant therapy is a plausible method for treatment of these diseases. The studies will test our hypothesis that the mice that have low antioxidant levels would be vulnerable to the diseases related to

reactive oxygen species (ROS) and these mice would benefit greatly from antioxidant intervention. The hypothesis will be strengthened by exogenous lipoic acid (LA) administration. On the other hand, mice with an enhanced antioxidant reservoir are more resistant to ROS and should retard the development of the diseases. LA is a powerful antioxidant produced by lipoic acid synthase (Lias) in mitochondria, and a cofactor in several mitochondrial enzyme complexes such as pyruvate dehydrogenase complex and α -ketoglutarate dehydrogenase complex, which both participate in glucose oxidation and ATP generation. The 3'-untranslated region (3'-UTR) sequences play an important role in determining mRNA stability and influence final protein levels. We have generated mouse models under- and over-expressing the Lias gene by replacing the 3'-UTR of the Lias gene with c-Fos 3'-UTR or bovine growth hormone (bGH) 3'-UTR produced by homologous recombination in embryonic stem cells. These mice initially produce stabilized transcripts of the Lias gene using the 3'UTR sequence of bGH, but change to unstable transcripts using the 3'UTR from the cFos gene after Cre-mediated recombination is induced. The Liashigh/+ mice are crossed with Tg (Ella-cre) mice that express Cre-recombinase in testis and thus the offspring (Liaslow/+) express low levels of Lias. LiasLow/Low and Liashigh/high mice display approximately 25% and 150% of Lias gene expression, respectively, compared with wild type mice. These mutant mice also exhibit correspondingly altered endogenous antioxidant capacity and oxidative stress levels that are consistent, reliable and heritable. The novel antioxidant mouse models will be mated with disease mouse models. The double mutant mouse models will be used to quantify the impact of predisposed graded antioxidant baseline levels on the development of the diseases. Currently, there is no appropriate antioxidant mouse model available to test this possibility in preclinical studies. The novel Lias mouse model will fill this gap. The model will have a broad application for many ROS-related diseases upon being crossed with different disease models and

provide an appropriate preclinical platform to develop new antioxidant therapeutic strategies. Note: *the authors have equal contribution Acknowledgment: This project is supported by the National Natural Science Foundation of China (NSFC: 81370916) Xianwen Yi Professor of Public Health School of Public Health Xinxiang Medical University Xinxiang, Henan Province, 453003 xyi2000@hotmail.com

Article ID: 40184

Title: KeyGene's Green Gene Revolution: molecular mutagenesis for plant breeding

Name: Michiel van Eijk

Affiliation: KeyGene

E-mail: mzi@keygene.com

Abstract

During the last 50 years plant breeding has resulted in enormous improvements of crops in terms of yield, quality, resistances and appearance of our agricultural products. However, the pace of improvement is no longer in line with the rapidly increasing demand and traditional methods are reaching their limits. The growing world population requires significant improvements of crops to meet the future demands for high quality food, feed, fiber, fuel, flowers and fun (6F) agricultural products. KeyGene's passion is a Green Gene Revolution approach to explore and exploit existing and induced genetic variation in vegetable and other 6F crops. To realize our goals, KeyGene deploys technologies in the platforms Advanced Molecular Breeding, Molecular Mutagenesis and Lead Discovery, and focuses its research on (a)biotic stresses, herbicide tolerance and reproduction traits. I will present how KeyGene deploys its proprietary KeyBase and KeyPoint methods from the Molecular Mutagenesis platform to improve genes affecting crop traits. KeyBase is a genome-editing technology for oligo-nucleotide directed mutagenesis (ODM), allowing the creating of a single point mutation at a specific position in the target gene, while KeyPoint

technology uses Next-Generation Sequencing to screen large numbers of genes for random base changes in mutagenized or natural populations. Examples will be shown illustrating the power of these methods to accelerate trait improvement in a variety of vegetable and field crops. The KeyBase and KeyPoint technologies are protected by patents and patent applications owned by Keygene N.V. KeyBase and KeyPoint are registered trademarks of Keygene N.V.

Article ID: 40168

Title: Evaluation of Nasal Functions While Wearing N95 Respirator and Surgical Facemask

Name: Jian Hua Zhu

Affiliation: Dept. ME National University of Singapore

E-mail: jhzhu.me@gmail.com

Abstract

There is a lack of reported studies on how the long duration wearing of N95 respirators or surgical facemasks will affect the upper airway functions. Considering the frequency of mask wearing especially in hospitals and during an outbreak of influenza, it is essential to have such data documented. Therefore, the current study is to establish the effect of long duration wearing of N95 and surgical facemasks on upper airway functions. 47 staffs of National University Hospital Singapore in 2013 were recruited. Each of the volunteers wore both N95 respirator and surgical facemask for 3 hours on two different days. During the period of mask wearing, relative airflow rates were recorded. Smell function test was carried out before and after mask wearing. The results show that no significant change of smell test score was found after removal of both the two types of masks. With N95 respirator, more air was breathed into the upper airways compared to surgical facemask.

Article ID: 40173

Title: Attention Drawing of Movie Trailers Revealed

by Electroencephography Using Sample Entropy

Name: Po-Shan Wang

Affiliation: Taipei Municipal Gan-Dau Hospital

E-mail: b8001071@gmail.com

Abstract

A movie trailer is a common advertising tool in the entertainment industry. Detection of a viewer's brain responses to a movie trailer can help film producers to tailor a more appealing trailer of a movie. In this study, we acquired electroencephalographic (EEG) signals from subjects when they watched movie trailers (labeled as Movie session), and compared with their resting state session (labeled as Resting session) or when they watch nature scenes (labeled as Nature session). We used Sample Entropy (SampEn) to analyze the EEG signals between different sessions. Results showed that the complexity ratios at Fp1, Fp2 and Fz channels derived from Movie session were significantly lower than that in Resting state or when subjects watched Nature session ($p < 0.001$). Our results suggest that the brain status can affect the complexity of their EEG. Further, the attraction of attention of a movie trailer can be observed from the change of EEG.

Article ID: 40176

Title: Data Classification with Modified Density Weighted Distance Measure for Diffusion Maps

Name: Yu-Te Wu

Affiliation: National Yang-Ming University

E-mail: ytwu@ym.edu.tw

Abstract

Clinical data analysis is of fundamental importance, as classifications and detailed characterizations of diseases help physicians decide suitable management for patients, individually. In our study, we adopt diffusion maps to embed the data into corresponding lower dimensional representation, which integrate the information of potentially nonlinear progressions of the diseases. To deal with nonuniformity of the data, we also consider an alternative distance measure

based on the estimated local density. Performance of this modification is assessed using artificially generated data. Another clinical dataset that comprises metabolite concentrations measured with magnetic resonance spectroscopy was also classified. The algorithm shows improved results compared with conventional Euclidean distance measure.

Article ID: 40336

Title: Age-Related Changes in Probability Density Function of Pairwise Euclidean Distances between Multichannel Human EEG Signals

Name: Mikhail Trifonov

Affiliation: IEPB of the Russian Academy of Science

E-mail: mtrifonov@mail.ru

Abstract

The probability density functions (pdf's) and the first order structure functions (SF's) of the pairwise Euclidean distances between scaled multichannel human EEG signals at different time lags under hypoxia and in resting state at different ages are estimated. It is found that the hyper gamma distribution is a good fit for the empirically derived pdf in all cases. It means that only two parameters (sample mean of EEG Euclidean distances at a given time lag and relevant coefficient of variation) may be used in the approximate classification of empirical pdf's. Both these parameters tend to increase in the first twenty years of life and tend to decrease as healthy adults getting older. Our findings indicate that such age-related dependence of these parameters looks like as age-related dependence of the total brain white matter volume. It is shown that 15 min hypoxia (8% oxygen in nitrogen) causes a significant (about 50%) decreasing of the mean relative displacement EEG value that is typical for the rest state. In some sense the impact of the oxygen deficit looks like the subject getting older during short-term period.

Article ID: 40370

Title: Research on thermal effect of electrosurgery

with anti-adhesion composite films

Name: Han-Yi Cheng

Affiliation: Biomedical Materials and Tissue Engineering

E-mail: chytmu@gmail.com

Abstract

The purpose of this study is to investigate the thermal effect on the liver resulting from electro-surgical devices with copper-doped diamond-like carbon (a-C:H/Cu) surface treatment using computer aided analysis and animal models. It is necessary to reduce the thermal damage in the adjacent tissues for clinical electrosurgical surgeries. a-C:H/Cu films were characterized by scanning electron microscope (SEM) and transmission electron microscopy (TEM) to analyze the surface morphologies in this study. Bionic liver models were reconstructed using magnetic resonance image (MRI), and results indicated that the temperature decreased significantly when using electro-surgical device with nanostructured a-C:H/Cu films, temperature also decreased with increasing film thicknesses. Lesions were made on the liver of adult rats, and thermography revealed the surgical temperature in liver tissue from the a-C:H/Cu group was significantly lower than the un-treated group. Moreover, a-C:H/Cu electrodes caused a relatively smaller area of injury area and lateral thermal injury, a smaller area of fibrotic tissue, and a faster process of wound healing than the untreated group. Results indicated that the coated film reduced excessive temperature and transformed the temperature uniformly in the liver tissue.

Article ID: 40083

Title: A preliminary phantom study for post-reconstruction material separation using dual-energy micro-computed tomography

Name: Hsiang-Ling Huang

Affiliation: National Yang-Ming University

E-mail: sandradoo59@gmail.com

Abstract

Background Using dual-energy in micro-CT systems can provide sufficient information to resolve the density and composition of inspected objects and makes it possible to differentiate materials on the basis of their unique energy-dependent attenuation profiles.

Purpose The purpose of this study was to use dual-energy in our homemade micro-CT system to differentiate tissue composition with different dual-energy material decomposition approaches.

Materials and methods The physical experiments were performed on a laboratory homemade micro-CT system. The useful operating energy range was from 30 to 60 kV. We used a two-material phantom composed of 15% iodine-based contrast agent and water and both were put into 2-mL eppendorf tubes, respectively. The energy pair was set at 40 and 60 kV. Owing to the different attenuation characteristics of contrast agent and water, we could decompose two images taken at low and high energies into water-only and contrast-only images. The decomposition process was achieved by weighting subtraction and independent component analysis (ICA) methods. Additionally, in order to estimate these two compositions' volume fraction, we used image based decomposition method which can be expressed as a linear combination of the attenuation coefficients of the basic materials multiplied by their volume fractions with the CT voxel size constraint.

Results We transformed all post-reconstruction images including original images and decomposed images into binary images to do the image segmentation. After the recognition of these two materials, comparing the relative position of the two materials, the sensitivity of iodine contrast agent separation based on weighting subtraction technique was 76.59% and ICA method was 76.70%. The results showed that both of these two methods could separate individual component properly. Furthermore, the image based decomposition method could obtain the contrast agent and water volume fractions which were 1.03 and 1.05, respectively. According to the results, relative errors were 3% and 5%. Therefore, the image based decomposition method not only could estimate the volume fractions but also independently segment these

two materials.

Conclusion We demonstrated the feasibility of separating iodine-based contrast agent and water using the weighting subtraction and ICA methods for this phantom study. Furthermore, an image based decomposition based on the basis materials was also performed to yield good quantitative results.

Article ID: 40134

Title: Multimodality Molecular Imaging for Targeted Biopsy of Prostate Cancer

Name: Baowei Fei

Affiliation: Emory University / Georgia Institute of Technology

E-mail: bfei@emory.edu

Abstract

Multimodality molecular imaging is a promising technology for improving cancer detection and diagnosis. It is estimated that one in six men will be diagnosed with prostate cancer during their lifetime. Systematic transrectal ultrasound (TRUS)-guided prostate biopsy is considered the standard method for prostate cancer detection. Current biopsy techniques have a significant sampling error and a low sensitivity. To improve the cancer detection rate from the current standard of care, the development and evaluation of new biopsy technology is an active research area. Positron emission tomography (PET) can detect metabolic and functional information of cancer. By combining PET with three-dimensional (3D) ultrasound images, multimodality image-guided targeted biopsy has become a promising technology for improved detection and diagnosis of prostate cancer. At our institution, we developed a PET-directed, 3D ultrasound-guided biopsy system. The system uses: (i) Passive mechanical components for guiding, tracking, and stabilizing the position of a commercially available, end-firing, transrectal ultrasound probe; (ii) Software components for acquiring, storing, and reconstructing a series of real-time 2D TRUS images into a 3D image; and (iii) Software that segment the prostate in 3D TRUS

images and displays a model of the 3D scene to guide a biopsy needle in three dimensions. The system allows real-time tracking and recording of the 3D position and orientation of the biopsy needle as a physician manipulates the ultrasound transducer. A workstation system is used to register and fuse PET and ultrasound images. In order to use 3D models to guide the biopsy, segmentation of the prostate is a key component of the 3D ultrasound image-guided biopsy system. We developed an automatic method to segment the prostate in 3D TRUS images. This method utilizes Wavelet-based texture extraction technique followed by support vector machines (SVMs) to adaptively collect texture priors of prostates and non-prostate tissues and classify tissues in different sub-regions around the prostate boundary by statistically analyzing their textures using wavelet features. In order to incorporate PET into the 3D ultrasound-guided biopsy, image registration plays a key role in combining the two imaging multimodalities. We used computed tomography (CT) images as the bridge to register PET with TRUS because both PET and CT images are acquired from a combined PET/CT system. We developed and evaluate a non-rigid registration method for this particular application. The use of PET/ultrasound fusion targeted biopsies within the diagnostic pathway would result in an enhanced detection of clinically significant disease, fewer men diagnosed with clinically insignificant disease, fewer men biopsied overall, and fewer needle deployments; thus it could transform prostate cancer management and change clinical practice from “blind” to “targeted” biopsy. The new molecular image-guided biopsy system has been tested in human patients at our institution. The new molecular imaging technology and image-guided system can have an immediate impact on the healthcare of cancer patients.

Article ID: 40117

Title: Validation of an Intracranial Aneurysm Image Segmentation Method via use of Silicone Models

Name: SEN yuka

Affiliation: Macquarie University

E-mail: yuka.sen@mq.edu.au

Abstract

Patient-specific intracranial aneurysm morphology and haemodynamic analysis has seen increasing utilisation in clinical applications for aneurysm formation and rupture. Segmentation technology is thus one of the fundamental technologies necessary to reconstruct vascular geometries from medical images; e.g. computed tomography (CT) angiography, magnetic resonance (MR) angiography, and digital subtraction (DS) angiography. However, though based on the same set of medical imaging data, the results of geometry and volume of intracranial aneurysms are highly dependent upon segmentation algorithms and may vary accordingly with the experience of the operators. In this study, we performed a series of in-vitro validation tests via the use of patient-specific silicone aneurysm models. These silicone models were scanned by 3D CT with four different dilution rates of contrast agent. The outcomes were then applied to validate our previously proposed segmentation method; Threshold-Based Level Set (TLS). These results were likewise employed to investigate optimal parameter settings for the best segmentation results. Four different types of silicone aneurysm models were designed for this study. In order to compare the results from different segmentation methods, another two segmentation methods; Region Growing Threshold (RGT), and Chan-Vese model (CV), were introduced to reconstruct the silicone model images. The results were evaluated via the use of parameters; the measurement of arterial volume differences (VD), Jaccard's measure (volume overlaps metric, JM), Hausdorff distance (maximum surface distance, HD) and mean absolute surface distance (MASD). Results obtained show that at the highest contrast solution (with a dilution of 1:5; one part contrast agent to four parts water), all segmentation methods achieved an overlap rate of more than 93% and less than 0.07 MASD. Even at the lowest contrast dilution (1:40), the TLS method is able to achieve an overlap of 89% with a MASD that is less than 0.12. The same results were

obtained via the use of a semi-manual RGT method, performed by an experienced operator, with results indicating that the TLS method provided a relatively stable geometry at various contrast densities. The study validated the accuracy of the proposed TLS segmentation method and discussed the optimal parameter settings for automatic segmentation. The TLS method is thus a valuable tool for clinical diagnosis and surgical preparation, and will furthermore, play a vital role as an important tool for future haemodynamic research.

Article ID: 40003

Title: Linkage Study of Autosomal Recessive Nonsyndromic Primary Microcephaly in Pakistani Kindered

Name: Saba Irshad

Affiliation: Punjab University

E-mail: saba.ibb@pu.edu.pk

Abstract

Microcephaly is heterogeneous, autosomal recessive trait with reduced head circumference of at least 4 SD below age and sex means due to reduction in neuron production. The brain of microcephalic patient is architecturally normal but severe to mild mental retardation. It is rare disease affecting 2-2.5% of total population specifically in Asia and Arab where the incidence of cousin marriages is relatively high. From seven known currently mapped loci ASPM is found to be the frequent causative agent. In the current investigations exclusion mapping of a microcephalic family was done. DNA from all blood samples was extracted using standard procedure and after gene specific PCR amplifications, 8% non-denaturing PAGE was done. Linkage was observed at MCPH5 locus where ASPM is a candidate gene on chromosome 1q31. The results of DNA sequencing showed G to A transition and Leucine (CTG) to Leucine (CTA) was noted. There are six triplet codons which differ by single nucleotide encoding for Leucine. Hence, no overall change in the effect of protein expression was observed due to the degeneracy of codons. Therefore, the sequencing of

the entire ASPM gene with intervening sequences was suggested in order to find the actual cause of microcephaly.

Article ID: 40281

Title: DNA methylation patterns and expression of DNMT1 in rheumatoid arthritis

Name: Attya Bhatti

Affiliation: Atta-ur Rahman School of Applied Biosciences, Nation

E-mail: attyabhatti@gmail.com

Abstract

Rheumatoid arthritis is an autoimmune disease with a characteristic of relentless synovitis, systemic inflammation and auto-antibodies. This patho-physiological condition is developed by genetic, epigenetic and environmental factors. Epigenetic is inherited change in regulation of gene expression without changing in sequence of DNA which includes DNA methylation and histone modification. DNA methylation has role in changing the expression level of gene by blocking the binding of transcription factor with promoter region. Therefore, it was aimed to detect methylation level in the promoter region of DNMT1 gene in rheumatoid arthritis and matching controls to compare the methylation level with mRNA expression of DNMT1 gene and to check association of DNMT1 gene with rheumatoid arthritis. DNA methylation level in the promoter region of DNMT1 gene was detected by methylation specific PCR and mRNA expression level was detected by real time PCR. Methylation level was compared with mRNA expression in cases and controls. The promoter region of DNMT1 was found methylated in rheumatoid arthritis and unmethylated in control. Moreover, the expression level of mRNA of DNMT1 gene was found less in patient as compared to control. Less than one fold change decrease was found in expression of mRNA in patient with respect to control. Therefore, it is concluded that the methylated promoter may contribute in the low expression of DNMT1 gene in patient and may be involved in the progression of rheumatoid arthritis.

Instructions for Presentations

Devices Provided by the Conference Organizing Committee:

- Laptops (with MS-office & Adobe Reader)
- Projectors & Screen
- Laser Sticks

Materials Provided by the Presenters:

- PowerPoint or PDF files

Duration of each Presentation:

- Oral Presentation: 10 -15 Minutes of Presentation, 5 Minutes of Q & A
- Invited Speech: 30 - 40 Minutes of Presentation, 5 Minutes of Q & A

Hotel Information

About Hotel

Located in Beijing's Zhongguancun Hi-tech Zone, the "Silicon Valley of China", Beijing Yanshan Hotel is in the neighbourhood of the North Third Ring Road and the Zhongguancun Street with convenient transport to the Capital Airport, Beijing Railway Station, National Library, Beijing TV Station and Shangdi Information Industry Base. Peking University, Qinghua University, Renmin University and many other famous universities as well as scientific and technical institutions are all in the vicinity. The Summer Palace and Yuanmingyuan — China's ancient royal gardens can be reached in several minutes' drive.

Address: No.38 A, Zhongguancun Street, Haidian District, Beijing

中国北京市海淀区中关村大街甲38号 (100086)

Homepage: <http://www.yanshanhotel.com/>

Telephone: (+86) 10 62563388

Facsimile: (+86) 10 62568640

How to Get to the Hotel

Please show the following message to the taxi driver if you cannot speak Chinese:

请送我到: 北京市海淀区中关村大街甲38号燕山大酒店

Contact Us

Secretary of Organizing Committee: Ms. Rollin

Telephone: +86-15172479625